

Published by Faculty of Sciences and Mathematics, University of Niš, Serbia Available at: http://www.pmf.ni.ac.rs/filomat

# A fractional stochastic model for aerosol transmission of fluid droplets and virus exposure in closed spaces

Dora Selešia, Stefan Tošićb,\*

<sup>a</sup>Department of Mathematics and Informatics, Faculty of Sciences, University of Novi Sad, Novi Sad, Serbia <sup>b</sup>Department of Fundamental Sciences, Faculty of Technical Sciences, University of Novi Sad, Novi Sad, Serbia

**Abstract.** Considering fractional Brownian motion  $B_t^H$  and fractional white noise  $W_t^H$  as a generalized stochastic processes in the framework of white noise analysis, we use them to model aerosol transmission of fluid droplets and virus exposure in closed space. The model is based on an airflow produced during coughing or sneezing governed by the incompressible Navier-Stokes equation, leading to the expulsion of contaminated aerosols that diffuse in a closed room and are subjected to random movements due to collision with other particles in the air. The proposed model involves stochastic components to grasp the uncertain nature of the aerosol diffusion and fractional derivatives to grasp the possibilities of a sub-diffusion or super-diffusion effect due to various physical conditions in the room. We prove existence and uniqueness of the solution to the proposed model, supported by numerical simulations and experiments.

#### Introduction

The problem of turbulent aerosol transmission of fluid droplets in a jet or puff, turned out to be very important in many areas of science and engineering after the global pandemic caused by the COVID-19 infection. Many papers have dealt with various models to describe the diffusion of contaminated aerosols in a coffined space, e.g. closed rooms or cabins in transport vehicles, [7], [10], [11], [12], [28], [29], [40], [41], [44], [46], [50], [51], [52], [53], to enlist just a few of them. Due to the now endemic nature of the SARS-CoV-2 virus with constantly upcoming new mutations that might break the vaccination barrier or other respiratory viruses lurking to cause a new global pandemic, it is of utmost importance to develop novel models that are capable of grasping both the inherent stochastic nature of the aerosol diffusion and the divergence from a normal diffusion. Stochastic partial differential equations (SPDEs) arise therefore as a natural context compared to deterministic PDEs to capture the random phenomena that influence the virus-containing droplets' diffusion. The framework of white noise analysis [20] and Wiener-Itô chaos expansion methods [21] has proven as a powerful tool for solving SPDEs; some techniques related to a

<sup>2020</sup> Mathematics Subject Classification. Primary 60H40; Secondary 60G20, 65C30, 76R50, 76M35, 76D05, 26A33, 35R11.

Keywords. Hermite polynomial, Navier-Stokes equations, chaos expansion, diffusion, Caputo-Fabrizio operators, fractional Brownian motion.

Received: 10 March 2025; Revised: 12 May 2025; Accepted: 15 May 2025

Communicated by Miljana Jovanović

The paper was supported by the Ministry of Education, Science and Technological Development, Republic of Serbia.

<sup>\*</sup> Corresponding author: Stefan Tošić

Email addresses: dora@dmi.uns.ac.rs (Dora Seleši), stefan.tosic@uns.ac.rs (Stefan Tošić)

 $ORCID\ iDs:\ https://orcid.org/0000-0003-2261-0590\ (Dora\ Seleši), https://orcid.org/0000-0002-3036-3289\ (Stefan\ Tošić)$ 

more direct approach avoiding complex transformations and relying on a coefficient-based calculation can be found in [13], [24], [25], [27], [31], and the references cited therein. A recent study has developed fractional Wiener-Hermite chaos expansions [16] for stochastic models with fractional Brownian motion. Another nuanced understanding of virus-contaminated aerosol dispersion leads to the fact that ordinary derivatives might not be optimal to describe these models. Fractional order derivatives can introduce a temporal element that captures the memory-dependent behavior of aerosol particles within the given environment, which enables the representation of diffusion processes that might deviate from a normal diffusion. Fractional order derivatives have a long-standing tradition not just as a well-studied theory but also as an important modeling tool in mechanics, engineering and material science [4], [32], [36], as well as in compartmental models used in epidemiology, sociology and computer science [1], [2], [14], [22], [35], to name only a few of them. In context of aerosol transmission, fractional derivatives allow for the inclusion of memory-related behaviors, such as the persistence of droplet movement or the prolonged influence of initial conditions. Allowing for a more realistic representation of the long-term behavior of droplets is particularly relevant in scenarios where air currents might not dissipate droplets quickly. The fractional order can capture the rate at which droplets disperse over an extended period, providing insights into potential exposure risks over time. By carefully choosing the order of the fractional derivative to be greater than one or less than one, it is possible to incorporate the effect of superdiffusion and subdiffusion, respectively, into the model. Superdiffusion occurs when particles spread more quickly than predicted by classical diffusion. In the context of virus-laden droplet dispersion in a closed room, superdiffusion might manifest as droplets covering larger distances than expected over a given time period. This behavior can be attributed to factors like the presence of strong air currents or irregular airflow patterns. Subdiffusion, on the other hand, entails slower particle spreading compared to classical diffusion. It is often observed when particles encounter obstacles, adhere to surfaces, or experience confinement, that might correspond to a reduced rate of droplet movement due to interactions with surfaces, corners, or air stagnation. There exist many definitions of a fractional derivative starting from the classical Riemann-Liouville and Caputo ones up to novel ones [48]. A recent type of fractional derivative is the Caputo-Fabrizio derivative [4], [8], [30], [43], that has a non-singular kernel and allows to reduce the fractional order derivative to an integer order derivative in PDEs. The Caputo-Fabrizio derivative has been used in many applications modeling the spread of viruses within population or other medical effects [3], [23], [38], [47], [49].

This paper aims to provide a model of a two-phase mixture of liquid droplets dispersed into an unsteady turbulent airflow caused by a violent expiratory event, such as coughing and sneezing. We will consider aerosol transmission within a finite time frame [0,T] in a cube-shaped closed room centered in the origin  $[-L,L]^3$ . The model is described as a set of well-known equations with respect to velocity U(t) and position X(t) of a droplet, but unlike the standard approach (see [34]), our model is enriched with the Caputo-Fabrizio fractional derivative instead of the ordinary derivative with respect to the time variable. Moreover, we suppose that each droplet is affected by some unpredictable airflows or collisions with air-molecules and other particles, which are simulated by adding a fractional Brownian motion  $B_t^H$  to the equations of the model. Independently of that, the velocity of airflow exhaled from mouth during expulsion u = (u, v, w), is ruled by the incompressible Navier-Stokes equations. Since it is known that exhaled air during coughing or sneezing makes a flow with extremely high Reynolds number (i.e. fully turbulent flow), we assume that it follows the so-called Trkal flow. Such an assumption, which means that vorticity and velocity fields are aligned, i.e.  $\partial \times u = u$ , could seem as a strong simplification, but it has turned out to be a reasonable choice in situations where we deal with incompresssible and turbulent flow fields. In contrast to recent papers (for instance see [40]) whose approach was to find numerical solution of the considered system, we are looking for a solution in form of the Wiener-Itô chaos expansion, i.e.

$$P(t,\omega) = (\mathbf{U}(t,\omega), \mathbf{X}(t,\omega))^T = \sum_{\alpha \in I} P_\alpha(t) H_\alpha(\omega),$$

where  $P_{\alpha}(t) \in C^1([0,T],[-L,L]^6)$ , for T,L > 0, and  $\omega \in S'(\mathbb{R})$ . Our main result is the theorem (supported by several appropriate lemmas) that guarantees the existence and uniqueness of a solution  $P(t,\omega)$ , in the space  $C([0,T],[-L,L]^6) \otimes (FS)'$  that was introduced in [26]. In order to achieve these results, first we apply white

noise analysis ([20], [21]) and consider chaos expansion of fractional white noise and fractional Brownian motion [33] in the form  $W^H(t,\omega) = \sum_{k=1}^{\infty} \sum_{j=1}^{\infty} b_{j,k} \xi_j(t) \langle \omega, \xi_k \rangle$  and  $B^H(t,\omega) = \sum_{k=1}^{\infty} \sum_{j=1}^{\infty} c_{j,k} \xi_j(t) \langle \omega, \xi_k \rangle$ , where coefficients  $b_{j,k}$  and  $c_{j,k}$  are given in Appendix (C), while  $\xi_j$  denotes the jth Hermite function and  $H \in (0,1)$  is the Hurst parameter. These results are in detail derived in [42] and might be of independent interest for readers who need algorithms for the simulation of fractional Brownian motion or fractional white noise, since they are novel and rely on computing the coefficients in a recursive manner. In the next step we utilize those coefficients to calculate the coefficients of the chaos expansion representation of the solution  $P(t,\omega)$ , and ultimately to provide some numerical approximations by truncating the infinite series. We also provide error estimates for the truncated series to validate the numerical approximation. Finally, we validate the model by comparing our model and the obtained simulation of aerosol trajectories with several realistic scenarios of expiratory events and photographs of aerosol clouds obtained from [17].

In conclusion we note that there is a vast literature on aerosol dispersion models that use only a theoretical approach with no model validation (e.g. [37], [39]), as well as a large number of papers that deal with various software-based simulation techniques (e.g. [40], [50]), closer to reality but again without a model validation. Our paper has the advantage that it not only develops a novel theoretical model and provides simulations for several parameter scenarios, but also validates the model on a realistic database.

The paper is organized as follows:

Section 1 contains the main results of this paper and is devoted to the aerosol transmission model as described above, and to proving the existence and uniqueness of the solution to the underlying fractional stochastic system in an appropriate space of generalized stochastic processes. In Section 2 we provide some numerical simulations of the approximate solutions to illustrate our results. An interesting result is that the approximations are verified by an error estimate on the truncation of the chaos expansion series to a finite sum, which can be expressed via the Hurwitz zeta function. Simulations are given for different fractional orders of the Caputo-Fabrizio derivative, as well as different values of the Hurst parameter  $H \in (0,1)$ . In Section 3 we compare our model with some realistic scenarios of aerosol diffusion based on an open database of expiratory images and videos. All results in Sections 1–3 are original and novel. The Appendix at the end contains details on the theoretical framework on Wiener-Itô chaos expansions, Caputo-Fabrizio calculus, formulae regarding the Hermite polynomials and functions, as well as an explanation of feasible physical parameters that were used in the simulation of aerosol diffusion.

## 1. A fractional stochastic model for the droplet diffusion dynamics

In a recent paper [40], the airflow, exhaled from the mouth during a human cough, was ruled by the incompressible Navier-Stokes equations given by

$$\partial_t u + u \cdot \partial u = -\frac{1}{\rho_a} \partial p + \nu \partial^2 u, \quad \partial \cdot u = 0, \tag{1}$$

with  $\nu$  being the air kinematic viscosity and  $\rho_a$  the air density. It is known that exhaled air during expulsion makes a flow with extremely high Reynolds number, and the flow field is thus fully turbulent which causes a number of problems from a numerical point of view. In our model the air during expulsion is assumed to follow a Trkal flow, which means that vorticity and velocity fields are aligned, i.e.  $\partial \times u = u$ . Such an assumption has proven as an reasonable choice in situations where we deal with incompressible and turbulent flow fields. Hence, we consider a particular form of the exact solution of 3-D Navier-Stokes equations given in [5],

$$u = (A\sin(kz) + C\cos(ky))e^{-\nu k^2 t},$$

$$v = (B\sin(kx) + A\cos(kz))e^{-\nu k^2 t},$$

$$w = (C\sin(ky) + B\cos(kx))e^{-\nu k^2 t},$$
(2)

and

$$p = -\rho_a \Big( BC \cos(kx) \sin(ky) + AB \sin(kx) \cos(kz) + AC \sin(kz) \cos(ky) \Big) e^{2\nu k^2 t},$$

where A, B, C and k are arbitrary constants, while u = (u, v, w) and  $(x, y, z) \in \mathbb{R}^3$ .

Taking system of deterministic equations considered in [40] as a starting point, we are now ready to introduce our model for the dynamics of an individual droplet exhaled from the mouth during coughing. It is the system of fractional stochastic differential equations with fractional Brownian motion given by

$${}^{CF}D^{\alpha}\boldsymbol{U}(t,\omega) = \frac{\boldsymbol{u}^{\diamond}(\boldsymbol{X}(t,\omega),t) - \boldsymbol{U}(t,\omega)}{\tau} + \sqrt{2\kappa_{1}}\boldsymbol{B}^{H}(t,\omega) - \boldsymbol{r}_{1}^{0}(t,\omega), \quad \boldsymbol{U}(0) = \boldsymbol{U}^{0}(\omega),$$

$${}^{CF}D^{\alpha}\boldsymbol{X}(t,\omega) = \boldsymbol{U}(t,\omega) + \sqrt{2\kappa_{2}}\boldsymbol{B}^{H}(t,\omega) - \boldsymbol{r}_{2}^{0}(t,\omega), \quad \boldsymbol{X}(0) = \boldsymbol{X}^{0}(\omega),$$

$$(3)$$

where  $\mathfrak{a} \in [0,1]$  is the order of the Caputo-Fabrizio fractional derivative, and  $\kappa_1$  and  $\kappa_2$  are Brownian diffusivity constants, whose sum is equal to the water vapor diffusivity  $D_{\nu}$  in the limit of tracer particles,  $\tau \to 0$ . The vector  $X(t,\omega) = (X(t,\omega),Y(t,\omega),Z(t,\omega))$  represents the position of droplet, while  $U(t,\omega) = (U(t,\omega),V(t,\omega),W(t,\omega))$  represents its velocity. The last terms  $r_1^0(t,\omega)$  and  $r_2^0(t,\omega)$  are regularization terms, that are required to make the problem well-posed in Caputo-Fabrizio sense (see Appendix E), respectively given by

$$\mathbf{r}_{1}^{0}(t,\omega) = \frac{\left(\mathbf{u}^{\diamond}(\mathbf{X}^{0}(\omega),0) - \mathbf{U}^{0}(\omega)\right)}{\tau} e^{-\frac{\alpha}{1-\alpha}t},$$
  
$$\mathbf{r}_{2}^{0}(t,\omega) = \mathbf{U}^{0}(\omega)e^{-\frac{\alpha}{1-\alpha}t}.$$

These terms introduce an effect that vanishes as  $t \to \infty$ , so that the regularization has a larger effect at initial time t=0 where the Caputo-Fabrizio derivative must be equal to zero, while at later time-points this effect becomes negligible and the fractional Brownian motion takes over to have greater influence on the diffusion. The function  $u^{\Diamond}(X(t,\omega),t) = (u^{\Diamond}(X(t,\omega),t),v^{\Diamond}(X(t,\omega),t),w^{\Diamond}(X(t,\omega),t))$  is the Wick version of the analytical Trkal solution of the 3-D incompressible Navier-Stokes equations given by

$$u^{\diamond}(X(t,\omega),t) = (A\sin^{\diamond}(kZ(t,\omega)) + C\cos^{\diamond}(kY(t,\omega)))e^{-\nu k^{2}t},$$

$$v^{\diamond}(X(t,\omega),t) = (B\sin^{\diamond}(kX(t,\omega)) + A\cos^{\diamond}(kZ(t,\omega)))e^{-\nu k^{2}t},$$

$$w^{\diamond}(X(t,\omega),t) = (C\sin^{\diamond}(kY(t,\omega)) + B\cos^{\diamond}(kX(t,\omega)))e^{-\nu k^{2}t}.$$

Details related to the Caputo-Fabrizio derivative are given in Appendix E while for the Wick product and Wick version of analytic functions we refer to Appendix C at the end of this paper. The stochastic process  $B^H(t,\omega)$  is the 3-D fractional Brownian motion [21] defined by

$$B^{H}(t,\omega) = \Big(\sum_{j=1}^{\infty} \frac{1}{\Gamma(H+\frac{1}{2})} \int_{0}^{t} \frac{d}{ds} \int_{-\infty}^{s} \xi_{j}(\tau)(s-\tau)^{H-\frac{1}{2}} d\tau ds H_{\epsilon^{(1+3(j-1))}}(\omega),$$

$$\sum_{j=1}^{\infty} \frac{1}{\Gamma(H+\frac{1}{2})} \int_{0}^{t} \frac{d}{ds} \int_{-\infty}^{s} \xi_{j}(\tau)(s-\tau)^{H-\frac{1}{2}} d\tau ds H_{\epsilon^{(2+3(j-1))}}(\omega),$$

$$\sum_{j=1}^{\infty} \frac{1}{\Gamma(H+\frac{1}{2})} \int_{0}^{t} \frac{d}{ds} \int_{-\infty}^{s} \xi_{j}(\tau)(s-\tau)^{H-\frac{1}{2}} d\tau ds H_{\epsilon^{(3)}}(\omega)\Big).$$
(4)

We are looking for a solution to (3) as a generalized stochastic processes  $U(t, \omega) \in [-L_1, L_1]^3 \otimes (FS)'$  and  $X(t, \omega) \in [-L_2, L_2]^3 \otimes (FS)'$  which are represented as

$$U(t,\omega) = \sum_{\alpha \in I} U_{\alpha}(t) H_{\alpha}(\omega), \quad X(t,\omega) = \sum_{\alpha \in I} X_{\alpha}(t) H_{\alpha}(\omega), \quad t \in [0,T], \quad \omega \in \Omega,$$
(5)

(7)

where  $X_{\alpha}(t) = (X_{\alpha}(t), Y_{\alpha}(t), Z_{\alpha}(t))$ , and  $U_{\alpha}(t) = (U_{\alpha}(t), V_{\alpha}(t), W_{\alpha}(t))$ . Details on chaos expansions and the definition of the space (*FS*)' are given in Appendix C. Applying the Caputo-Fabrizio fractional integral to both equations of our model (3), and using the fact that  ${}^{CF}I^{\alpha}(r_1^0(t,\omega)) = 0$ ,  ${}^{CF}I^{\alpha}(r_2^0(t,\omega)) = 0$  we obtain

$${^{CF}I^{\alpha}}({^{CF}D^{\alpha}}\boldsymbol{U}(t,\omega)) = \frac{{^{CF}I^{\alpha}}\boldsymbol{u}^{\Diamond}(\boldsymbol{X}(t,\omega),t) - {^{CF}I^{\alpha}}\boldsymbol{U}(t,\omega)}{\tau} + \sqrt{2\kappa_{1}}{^{CF}I^{\alpha}}\boldsymbol{B}^{H}(t,\omega),$$

$${^{CF}I^{\alpha}}({^{CF}D^{\alpha}}\boldsymbol{X}(t,\omega)) = {^{CF}I^{\alpha}}\boldsymbol{U}(t,\omega) + \sqrt{2\kappa_{2}}{^{CF}I^{\alpha}}\boldsymbol{B}^{H}(t,\omega),$$

which by using definition (E.2) and the identity (E.3) results in

$$\begin{split} \boldsymbol{U}(t,\omega) - \boldsymbol{U}(0,\omega) &= \frac{1-\mathfrak{a}}{\tau} [\boldsymbol{u}^{\Diamond}(\boldsymbol{X}(t,\omega),t) - \boldsymbol{u}^{\Diamond}(\boldsymbol{X}(0,\omega),0)] + \frac{\mathfrak{a}}{\tau} \int_{0}^{t} \boldsymbol{u}^{\Diamond}(\boldsymbol{X}(s,\omega),s) ds - \\ &\quad - \frac{1-\mathfrak{a}}{\tau} [\boldsymbol{U}(t,\omega) - \boldsymbol{U}(0)] - \frac{\mathfrak{a}}{\tau} \int_{0}^{t} \boldsymbol{U}(s,\omega) ds + \\ &\quad + \sqrt{2\kappa_{1}}(1-\mathfrak{a})[\boldsymbol{B}^{H}(t,\omega) - \boldsymbol{B}^{H}(0,\omega)] + \sqrt{2\kappa_{1}}\mathfrak{a} \int_{0}^{t} \boldsymbol{B}^{H}(s,\omega) ds, \\ \boldsymbol{X}(t,\omega) - \boldsymbol{X}(0,\omega) &= (1-\mathfrak{a})[\boldsymbol{U}(t,\omega) - \boldsymbol{U}(0,\omega)] + \mathfrak{a} \int_{0}^{t} \boldsymbol{U}(s,\omega) ds + \\ &\quad + \sqrt{2\kappa_{2}}(1-\mathfrak{a})[\boldsymbol{B}^{H}(t,\omega) - \boldsymbol{B}^{H}(0,\omega)] + \sqrt{2\kappa_{2}}\mathfrak{a} \int_{0}^{t} \boldsymbol{B}^{H}(s,\omega) ds. \end{split}$$

Finally, after differentiating both equations with respect to t, the model obtains a new interesting form on the right hand side, as a convex combination of the first order derivatives and the zeroth order derivatives, giving the Caputo-Fabrizio fractional order operator a natural interpretation as an interpolated derivative:

$$\mathbf{U}'(t,\omega) = (1-\mathfrak{a})\frac{d}{dt} \left[ \frac{\mathbf{u}^{\diamond}(\mathbf{X}(t,\omega),t) - \mathbf{U}(t,\omega)}{\tau} + \sqrt{2\kappa_1}\mathbf{B}^H(t,\omega) \right] + \\
+ \mathfrak{a} \left[ \frac{\mathbf{u}^{\diamond}(\mathbf{X}(t,\omega),t) - \mathbf{U}(t,\omega)}{\tau} + \sqrt{2\kappa_1}\mathbf{B}^H(t,\omega) \right], \quad \mathbf{U}(0) = \mathbf{U}^0(\omega), \\
\mathbf{X}'(t,\omega) = (1-\mathfrak{a})\frac{d}{dt} \left[ \mathbf{U}(t,\omega) + \sqrt{2\kappa_2}\mathbf{B}^H(t,\omega) \right] + \\
+ \mathfrak{a} \left[ \mathbf{U}(t,\omega) + \sqrt{2\kappa_2}\mathbf{B}^H(t,\omega) \right], \quad \mathbf{X}(0) = \mathbf{X}^0(\omega). \tag{7}$$

By using (D.1) and (D.2) for all components of the Wick version of the analytical Trkal solution  $u^{\Diamond}(X(t,\omega),t)=$  $(u^{\diamond}(X(t,\omega),t),v^{\diamond}(X(t,\omega),t),w^{\diamond}(X(t,\omega),t))$  we rewrite all processes that figure in (6) and (7) in their corresponding Wiener-Itô chaos expansion form. For (6) we obtain the following equations

$$\sum_{\alpha \in I} U'_{\alpha}(t)H_{\alpha}(\omega) = (1 - \mathfrak{a})\frac{d}{dt} (g_{\alpha,U}(t) + h_{1}(t)) + \mathfrak{a} (g_{\alpha,U}(t) + h_{1}(t)),$$

$$\sum_{\alpha \in I} V'_{\alpha}(t)H_{\alpha}(\omega) = (1 - \mathfrak{a})\frac{d}{dt} (g_{\alpha,V}(t) + h_{1}(t)) + \mathfrak{a} (g_{\alpha,V}(t) + h_{1}(t)),$$

$$\sum_{\alpha \in I} W'_{\alpha}(t)H_{\alpha}(\omega) = (1 - \mathfrak{a})\frac{d}{dt} (g_{\alpha,W}(t) + h_{1}(t)) + \mathfrak{a} (g_{\alpha,W}(t) + h_{1}(t)),$$

$$\sum_{\alpha \in I} U_{\alpha}(0)H_{\alpha}(\omega) = \sum_{\alpha \in I} U^{0}_{\alpha}H_{\alpha}(\omega),$$

while the system (7) obtains the form

$$\sum_{\alpha\in\mathcal{I}}X'_{\alpha}(t)H_{\alpha}(\omega)=(1-\mathfrak{a})\frac{d}{dt}\left(\sum_{\alpha\in\mathcal{I}}U_{\alpha}(t)H_{\alpha}(\omega)+h_{2}(t)\right)+\mathfrak{a}\left(\sum_{\alpha\in\mathcal{I}}U_{\alpha}(t)H_{\alpha}(\omega)+h_{2}(t)\right),$$

$$\begin{split} &\sum_{\alpha\in I}Y_{\alpha}'(t)H_{\alpha}(\omega)=(1-\mathfrak{a})\frac{d}{dt}\left(\sum_{\alpha\in I}V_{\alpha}(t)H_{\alpha}(\omega)+h_{2}(t)\right)+\mathfrak{a}\left(\sum_{\alpha\in I}V_{\alpha}(t)H_{\alpha}(\omega)+h_{2}(t)\right),\\ &\sum_{\alpha\in I}Z_{\alpha}'(t)H_{\alpha}(\omega)=(1-\mathfrak{a})\frac{d}{dt}\left(\sum_{\alpha\in I}W_{\alpha}(t)H_{\alpha}(\omega)+h_{2}(t)\right)+\mathfrak{a}\left(\sum_{\alpha\in I}W_{\alpha}(t)H_{\alpha}(\omega)+h_{2}(t)\right),\\ &\sum_{\alpha\in I}X_{\alpha}(0)H_{\alpha}(\omega)=\sum_{\alpha\in I}X_{\alpha}^{0}H_{\alpha}(\omega), \end{split}$$

where

$$g_{\alpha,U}(t) = -\frac{1}{\tau} \sum_{\alpha \in I} U_{\alpha}(t) H_{\alpha}(\omega)$$

$$+ \frac{A}{\tau} \Big( \sin(kZ_{0}(t)) H_{0}(\omega) + \sum_{|\alpha| > 0} \Big( k \sin(\frac{\pi}{2} + kZ_{0}(t)) Z_{\alpha}(t) + r_{\alpha,\sin(kZ)}(t) \Big) H_{\alpha}(\omega) \Big) e^{-\nu k^{2}t}$$

$$+ \frac{C}{\tau} \Big( \cos(kY_{0}(t)) H_{0}(\omega) + \sum_{|\alpha| > 0} \Big( k \cos(\frac{\pi}{2} + kY_{0}(t)) Y_{\alpha}(t) + r_{\alpha,\cos(kY)}(t) \Big) H_{\alpha}(\omega) \Big) e^{-\nu k^{2}t} ,$$

$$g_{\alpha,V}(t) = -\frac{1}{\tau} \sum_{\alpha \in I} V_{\alpha}(t) H_{\alpha}(\omega)$$

$$+ \frac{B}{\tau} \Big( \sin(kX_{0}(t)) H_{0}(\omega) + \sum_{|\alpha| > 0} \Big( k \sin(\frac{\pi}{2} + kX_{0}(t)) X_{\alpha}(t) + r_{\alpha,\sin(kX)}(t) \Big) H_{\alpha}(\omega) \Big) e^{-\nu k^{2}t}$$

$$+ \frac{A}{\tau} \Big( \cos(kZ_{0}(t)) H_{0}(\omega) + \sum_{|\alpha| > 0} \Big( k \cos(\frac{\pi}{2} + kZ_{0}(t)) Z_{\alpha}(t) + r_{\alpha,\cos(kZ)}(t) \Big) H_{\alpha}(\omega) \Big) e^{-\nu k^{2}t} ,$$

$$g_{\alpha,W}(t) = -\frac{1}{\tau} \sum_{\alpha \in I} W_{\alpha}(t) H_{\alpha}(\omega)$$

$$+ \frac{C}{\tau} \Big( \sin(kY_{0}(t)) H_{0}(\omega) + \sum_{|\alpha| > 0} \Big( k \sin(\frac{\pi}{2} + kY_{0}(t)) Y_{\alpha}(t) + r_{\alpha,\sin(kY)}(t) \Big) H_{\alpha}(\omega) \Big) e^{-\nu k^{2}t} ,$$

$$+ \frac{B}{\tau} \Big( \cos(kX_{0}(t)) H_{0}(\omega) + \sum_{|\alpha| > 0} \Big( k \cos(\frac{\pi}{2} + kX_{0}(t)) X_{\alpha}(t) + r_{\alpha,\cos(kX)}(t) \Big) H_{\alpha}(\omega) \Big) e^{-\nu k^{2}t} ,$$

and for  $n \in \{1, 2\}$ ,

$$h_n(t) = \frac{\sqrt{2\kappa_n}}{\Gamma(H+\frac{1}{2})} \sum_{j=1}^{\infty} \int_0^t \frac{d}{ds} \int_{-\infty}^s \xi_j(\tau)(s-\tau)^{H-\frac{1}{2}} d\tau ds (H_{\epsilon^{(1+3(j-1))}}(\omega), H_{\epsilon^{(2+3(j-1))}}(\omega), H_{\epsilon^{(3j)}}(\omega)).$$

By applying the orthogonality of  $\{H_{\alpha}(\omega)\}_{\alpha\in\mathcal{I}}$  this system reduces to a system of infinitely many deterministic systems of ordinary differential equations:

1° for 
$$\alpha = \mathbf{0}$$
,

$$U'_{0}(t) = (1 - \alpha) \frac{d}{dt} \left[ -\frac{1}{\tau} U_{0}(t) + \frac{1}{\tau} e^{-\nu k^{2}t} \left( A \sin(kZ_{0}(t)) + C \cos(kY_{0}(t)) \right) \right]$$

$$+ \alpha \left[ -\frac{1}{\tau} U_{0}(t) + \frac{1}{\tau} e^{-\nu k^{2}t} \left( A \sin(kZ_{0}(t)) + C \cos(kY_{0}(t)) \right) \right]; \quad U_{0}(0) = U_{0}^{0},$$

$$V'_{0}(t) = (1 - \alpha) \frac{d}{dt} \left[ -\frac{1}{\tau} V_{0}(t) + \frac{1}{\tau} e^{-\nu k^{2}t} \left( B \sin(kX_{0}(t)) + A \cos(kZ_{0}(t)) \right) \right]$$

$$+ \alpha \left[ -\frac{1}{\tau} V_{0}(t) + \frac{1}{\tau} e^{-\nu k^{2}t} \left( B \sin(kX_{0}(t)) + A \cos(kZ_{0}(t)) \right) \right]; \quad V_{0}(0) = V_{0}^{0},$$

$$W'_{0}(t) = (1 - \alpha) \frac{d}{dt} \left[ -\frac{1}{\tau} W_{0}(t) + \frac{1}{\tau} e^{-\nu k^{2}t} \left( C \sin(kY_{0}(t)) + B \cos(kX_{0}(t)) \right) \right]$$

$$+\mathfrak{a}\left[-\frac{1}{\tau}W_{\mathbf{0}}(t)+\frac{1}{\tau}e^{-\nu k^{2}t}\left(C\sin(kY_{\mathbf{0}}(t))+B\cos(kX_{\mathbf{0}}(t))\right)\right];\quad W_{\mathbf{0}}(0)=W_{\mathbf{0}}^{0},$$

$$X'_{0}(t) = (1 - \alpha)U'_{0}(t) + \alpha U_{0}(t); \quad X_{0}(0) = X_{0}^{0};$$

$$Y'_{0}(t) = (1 - \alpha)V'_{0}(t) + \alpha V_{0}(t); \quad Y_{0}(0) = Y_{0}^{0};$$

$$Z'_{0}(t) = (1 - \alpha)W'_{0}(t) + \alpha W_{0}(t); \quad Z_{0}(0) = Z_{0}^{0};$$

$$(9)$$

with initial conditions  $U_0(0) = (U_0^0, V_0^0, W_0^0)$  and  $X_0 = (X_0^0, Y_0^0, Z_0^0)$ .

 $2^{\circ}$  for  $|\alpha| = 1$ , i.e.  $\alpha = \epsilon^{(i)}$ ,  $i \in \mathbb{N}$ ,

$$\begin{split} U_{\epsilon^{(j)}}'(t) &= \\ (1-\mathfrak{a}) \frac{d}{dt} \left[ -\frac{1}{\tau} U_{\epsilon^{(j)}}(t) + \frac{1}{\tau} e^{-\nu k^2 t} \left( A k \sin(\frac{\pi}{2} + k Z_0(t)) Z_{\epsilon^{(j)}}(t) + C k \cos(\frac{\pi}{2} + k Y_0(t)) Y_{\epsilon^{(j)}}(t) \right) \\ &\quad + \mathbf{1}_{i,1} \frac{\sqrt{2\kappa_1}}{\Gamma(H+\frac{1}{2})} \int_0^t \frac{d}{ds} \int_{-\infty}^s \xi_j(\tau) (s-\tau)^{H-\frac{1}{2}} d\tau ds \right] \\ &\quad + \mathfrak{a} \left[ -\frac{1}{\tau} U_{\epsilon^{(j)}}(t) + \frac{1}{\tau} e^{-\nu k^2 t} \left( A k \sin(\frac{\pi}{2} + k Z_0(t)) Z_{\epsilon^{(j)}}(t) + C k \cos(\frac{\pi}{2} + k Y_0(t)) Y_{\epsilon^{(j)}}(t) \right) \right. \\ &\quad + \mathbf{1}_{i,1} \frac{\sqrt{2\kappa_1}}{\Gamma(H+\frac{1}{2})} \int_0^t \frac{d}{ds} \int_{-\infty}^s \xi_j(\tau) (s-\tau)^{H-\frac{1}{2}} d\tau ds \right]; \quad U_{\epsilon^{(j)}}(0) = U_{\epsilon^{(j)}}^0, \\ V_{\epsilon^{(j)}}'(t) &= \\ (1-\mathfrak{a}) \frac{d}{dt} \left[ -\frac{1}{\tau} V_{\epsilon^{(j)}}(t) + \frac{1}{\tau} e^{-\nu k^2 t} \left( B k \sin(\frac{\pi}{2} + k X_0(t)) X_{\epsilon^{(j)}}(t) + A k \cos(\frac{\pi}{2} + k Z_0(t)) Z_{\epsilon^{(j)}}(t) \right) \right. \\ &\quad + \mathbf{1}_{i,2} \frac{\sqrt{2\kappa_1}}{\Gamma(H+\frac{1}{2})} \int_0^t \frac{d}{ds} \int_{-\infty}^s \xi_j(\tau) (s-\tau)^{H-\frac{1}{2}} d\tau ds \right] \\ &\quad + \mathfrak{a} \left[ -\frac{1}{\tau} V_{\epsilon^{(j)}}(t) + \frac{1}{\tau} e^{-\nu k^2 t} \left( B k \sin(\frac{\pi}{2} + k X_0(t)) X_{\epsilon^{(j)}}(t) + A k \cos(\frac{\pi}{2} + k Z_0(t)) Z_{\epsilon^{(j)}}(t) \right) \right. \\ &\quad + \mathbf{1}_{i,2} \frac{\sqrt{2\kappa_1}}{\Gamma(H+\frac{1}{2})} \int_0^t \frac{d}{ds} \int_{-\infty}^s \xi_j(\tau) (s-\tau)^{H-\frac{1}{2}} d\tau ds \right]; \quad V_{\epsilon^{(j)}}(0) = V_{\epsilon^{(j)}}^0, \end{split}$$

$$W_{\epsilon^{(j)}}(t) = (1 - \mathfrak{a}) \frac{d}{dt} \left[ -\frac{1}{\tau} W_{\epsilon^{(j)}}(t) + \frac{1}{\tau} e^{-\nu k^{2}t} \left( Ck \sin(\frac{\pi}{2} + kY_{0}(t)) Y_{\epsilon^{(j)}}(t) + Bk \cos(\frac{\pi}{2} + kX_{0}(t)) X_{\epsilon^{(j)}}(t) \right) \right. \\ \left. + \mathbf{1}_{i,0} \frac{\sqrt{2\kappa_{1}}}{\Gamma(H + \frac{1}{2})} \int_{0}^{t} \frac{d}{ds} \int_{-\infty}^{s} \xi_{j}(\tau) (s - \tau)^{H - \frac{1}{2}} d\tau ds \right]$$

$$\left. + \mathfrak{a} \left[ -\frac{1}{\tau} W_{\epsilon^{(j)}}(t) + \frac{1}{\tau} e^{-\nu k^{2}t} \left( Ck \sin(\frac{\pi}{2} + kY_{0}(t)) Y_{\epsilon^{(j)}}(t) + Bk \cos(\frac{\pi}{2} + kX_{0}(t)) X_{\epsilon^{(j)}}(t) \right) \right. \\ \left. + \mathbf{1}_{i,0} \frac{\sqrt{2\kappa_{1}}}{\Gamma(H + \frac{1}{2})} \int_{0}^{t} \frac{d}{ds} \int_{-\infty}^{s} \xi_{j}(\tau) (s - \tau)^{H - \frac{1}{2}} d\tau ds \right]; \quad W_{\epsilon^{(j)}}(0) = W_{\epsilon^{(j)}}^{0},$$

$$\begin{split} X'_{\epsilon^{(j)}}(t) = & (1-\mathfrak{a}) \frac{d}{dt} \left[ U_{\epsilon^{(j)}}(t) + \mathbf{1}_{i,1} \frac{\sqrt{2\kappa_{2}}}{\Gamma\left(H + \frac{1}{2}\right)} \int_{0}^{t} \frac{d}{ds} \int_{-\infty}^{s} \xi_{j}(\tau)(s-\tau)^{H-\frac{1}{2}} d\tau ds \right] \\ & + \mathfrak{a} \left[ U_{\epsilon^{(j)}}(t) + \mathbf{1}_{i,1} \frac{\sqrt{2\kappa_{2}}}{\Gamma\left(H + \frac{1}{2}\right)} \int_{0}^{t} \frac{d}{ds} \int_{-\infty}^{s} \xi_{j}(\tau)(s-\tau)^{H-\frac{1}{2}} d\tau ds \right]; \quad X_{\epsilon^{(j)}}(0) = X_{\epsilon^{(j)}}^{0}, \\ Y'_{\epsilon^{(j)}}(t) = & (1-\mathfrak{a}) \frac{d}{dt} \left[ V_{\epsilon^{(j)}}(t) + \mathbf{1}_{i,2} \frac{\sqrt{2\kappa_{2}}}{\Gamma\left(H + \frac{1}{2}\right)} \int_{0}^{t} \frac{d}{ds} \int_{-\infty}^{s} \xi_{j}(\tau)(s-\tau)^{H-\frac{1}{2}} d\tau ds \right] \\ & + \mathfrak{a} \left[ V_{\epsilon^{(j)}}(t) + \mathbf{1}_{i,2} \frac{\sqrt{2\kappa_{2}}}{\Gamma\left(H + \frac{1}{2}\right)} \int_{0}^{t} \frac{d}{ds} \int_{-\infty}^{s} \xi_{j}(\tau)(s-\tau)^{H-\frac{1}{2}} d\tau ds \right]; \quad Y_{\epsilon^{(j)}}(0) = Y_{\epsilon^{(j)}}^{0}, \\ Z'_{\epsilon^{(j)}}(t) = & (1-\mathfrak{a}) \frac{d}{dt} \left[ W_{\epsilon^{(j)}}(t) + \mathbf{1}_{i,0} \frac{\sqrt{2\kappa_{2}}}{\Gamma\left(H + \frac{1}{2}\right)} \int_{0}^{t} \frac{d}{ds} \int_{-\infty}^{s} \xi_{j}(\tau)(s-\tau)^{H-\frac{1}{2}} d\tau ds \right] \\ & + \mathfrak{a} \left[ W_{\epsilon^{(j)}}(t) + \mathbf{1}_{i,0} \frac{\sqrt{2\kappa_{2}}}{\Gamma\left(H + \frac{1}{2}\right)} \int_{0}^{t} \frac{d}{ds} \int_{-\infty}^{s} \xi_{j}(\tau)(s-\tau)^{H-\frac{1}{2}} d\tau ds \right]; \quad Z_{\epsilon^{(j)}}(0) = Z_{\epsilon^{(j)}}^{0}, \end{split}$$

where i=3(j-1)+l for  $j\in\mathbb{N}$ ,  $l\in\{0,1,2\}$ , while  $\mathbf{1}_{i,l}=1$  if  $i\equiv_3 l$ , otherwise it is zero. Initial conditions are given by  $\mathbf{U}_{\epsilon^{(i)}}(0)=(U^0_{\epsilon^{(i)}},V^0_{\epsilon^{(i)}},W^0_{\epsilon^{(i)}})$ , and  $\mathbf{X}_{\epsilon^{(i)}}(0)=(X^0_{\epsilon^{(i)}},Y^0_{\epsilon^{(i)}},Z^0_{\epsilon^{(i)}})$ .  $3^\circ$  for  $|\alpha|>1$ ,

$$(1-a)\frac{d}{dt}\left[-\frac{1}{\tau}U_{\alpha}(t) + \frac{1}{\tau}e^{-vk^{2}t}\left(Ak\sin(\frac{\pi}{2} + kZ_{0}(t))Z_{\alpha}(t) + Ck\cos(\frac{\pi}{2} + kY_{0}(t))Y_{\alpha}(t) + Ar_{\alpha,\sin(kZ)}(t) + Cr_{\alpha,\cos(kY)}(t)\right)\right]$$

$$+\alpha\left[-\frac{1}{\tau}U_{\alpha}(t) + \frac{1}{\tau}e^{-vk^{2}t}\left(Ak\sin(\frac{\pi}{2} + kZ_{0}(t))Z_{\alpha}(t) + Ck\cos(\frac{\pi}{2} + kY_{0}(t))Y_{\alpha}(t) + Ar_{\alpha,\sin(kZ)}(t) + Cr_{\alpha,\cos(kY)}(t)\right)\right]; \quad U_{\alpha}(0) = U_{\alpha}^{0},$$

$$V'_{\alpha}(t) = (1-a)\frac{d}{dt}\left[-\frac{1}{\tau}V_{\alpha}(t) + \frac{1}{\tau}e^{-vk^{2}t}\left(Bk\sin(\frac{\pi}{2} + kX_{0}(t))X_{\alpha}(t) + Ak\cos(\frac{\pi}{2} + kZ_{0}(t))Z_{\alpha}(t) + Br_{\alpha,\sin(kX)}(t) + Ar_{\alpha,\cos(kZ)}(t)\right)\right]$$

$$+\alpha\left[-\frac{1}{\tau}V_{\alpha}(t) + \frac{1}{\tau}e^{-vk^{2}t}\left(Bk\sin(\frac{\pi}{2} + kX_{0}(t))X_{\alpha}(t) + Ak\cos(\frac{\pi}{2} + kZ_{0}(t))Z_{\alpha}(t) + Br_{\alpha,\sin(kX)}(t) + Ar_{\alpha,\cos(kZ)}(t)\right)\right]; \quad V_{\alpha}(0) = V_{\alpha}^{0},$$

$$W'_{\alpha}(t) = (1-a)\frac{d}{dt}\left[-\frac{1}{\tau}W_{\alpha}(t) + \frac{1}{\tau}e^{-vk^{2}t}\left(Ck\sin(\frac{\pi}{2} + kY_{0}(t))Y_{\alpha}(t) + Bk\cos(\frac{\pi}{2} + kX_{0}(t))X_{\alpha}(t) + Cr_{\alpha,\sin(kY)}(t) + Br_{\alpha,\cos(kX)}(t)\right)\right]$$

$$+\alpha\left[-\frac{1}{\tau}W_{\alpha}(t) + \frac{1}{\tau}e^{-vk^{2}t}\left(Ck\sin(\frac{\pi}{2} + kY_{0}(t))Y_{\alpha}(t) + Bk\cos(\frac{\pi}{2} + kX_{0}(t))X_{\alpha}(t) + Cr_{\alpha,\sin(kY)}(t) + Br_{\alpha,\cos(kX)}(t)\right)\right]; \quad W_{\alpha}(0) = W_{\alpha}^{0},$$

with  $r_{\alpha,\Phi}(t)$  denoting the remainder terms of a Wick-analytical function  $\Phi$ , now taken as either the

sine or cosine function, as described in (D.2), and

$$X'_{\alpha}(t) = (1 - \alpha)U'_{\alpha}(t) + \alpha U_{\alpha}(t); \quad X_{\alpha}(0) = X^{0}_{\alpha},$$

$$Y'_{\alpha}(t) = (1 - \alpha)V'_{\alpha}(t) + \alpha V_{\alpha}(t); \quad Y_{\alpha}(0) = Y^{0}_{\alpha},$$

$$Z'_{\alpha}(t) = (1 - \alpha)W'_{\alpha}(t) + \alpha W_{\alpha}(t); \quad Z_{\alpha}(0) = Z^{0}_{\alpha},$$
(13)

with initial conditions  $U_{\alpha}(0) = (U_{\alpha I}^0 V_{\alpha I}^0 W_{\alpha I}^0)$  and  $X_{\alpha}(0) = (X_{\alpha I}^0 Y_{\alpha I}^0 Z_{\alpha I}^0)$ .

Now, we define the matrix valued functions S(t), N(t):  $\mathbb{R} \to \mathbb{R}^{6\times 6}$ , by

$$S(t) = \begin{bmatrix} \frac{1-\alpha+\tau}{\tau} & 0 & 0 & 0 & \frac{1-\alpha}{\tau} \frac{kC}{e^{\nu k^2 t}} \sin(kY_0(t)) & \frac{\alpha-1}{\tau} \frac{kA}{e^{\nu k^2 t}} \cos(kZ_0(t)) \\ 0 & \frac{1-\alpha+\tau}{\tau} & 0 & \frac{\alpha-1}{\tau} \frac{kB}{e^{\nu k^2 t}} \cos(kX_0(t)) & 0 & \frac{1-\alpha}{\tau} \frac{kA}{e^{\nu k^2 t}} \sin(kZ_0(t)) \\ 0 & 0 & \frac{1-\alpha+\tau}{\tau} & \frac{1-\alpha}{\tau} \frac{kB}{e^{\nu k^2 t}} \sin(kX_0(t)) & \frac{\alpha-1}{\tau} \frac{kC}{e^{\nu k^2 t}} \cos(kY_0(t)) & 0 \\ \alpha-1 & 0 & 0 & 1 & 0 & 0 \\ 0 & \alpha-1 & 0 & 0 & 1 & 0 \\ 0 & 0 & \alpha-1 & 0 & 0 & 1 \end{bmatrix},$$
(14)

$$N(t) = \begin{bmatrix} -\frac{\alpha}{\tau} & 0 & 0 & 0 & -\frac{\alpha}{\tau} \frac{C}{e^{\nu k^2 t}} \sin(kY_0(t)) & \frac{\alpha}{\tau} \frac{A}{e^{\nu k^2 t}} \cos(kZ_0(t)) \\ 0 & -\frac{\alpha}{\tau} & 0 & \frac{\alpha}{\tau} \frac{B}{e^{\nu k^2 t}} \cos(kX_0(t)) & 0 & -\frac{\alpha}{\tau} \frac{A}{e^{\nu k^2 t}} \sin(kZ_0(t)) \\ 0 & 0 & -\frac{\alpha}{\tau} & -\frac{\alpha}{\tau} \frac{B}{e^{\nu k^2 t}} \sin(kX_0(t)) & \frac{\alpha}{\tau} \frac{C}{e^{\nu k^2 t}} \cos(kY_0(t)) & 0 \\ \alpha & 0 & 0 & 0 & 0 & 0 \\ 0 & \alpha & 0 & 0 & 0 & 0 \\ 0 & 0 & \alpha & 0 & 0 & 0 & 0 \end{bmatrix}.$$
 (15)

The determinant of S(t) is equal to

$$Det(S(t)) = \frac{1}{\tau^3} \left[ (1 - \alpha + \tau)^3 + k^2 (1 - \alpha + \tau)(1 - \alpha)^4 e^{-2\nu k^2 t} \Big( BC \cos(kX_0(t)) \sin(kY_0(t)) + AB \cos(kZ_0(t)) \sin(kX_0(t)) + AC \cos(kY_0(t)) \sin(kZ_0(t)) \Big) + k^3 (1 - \alpha)^6 e^{-\frac{3\nu}{4} t} ABC e^{-3\nu k^2 t} \Big( \sin(kX_0(t)) \sin(kY_0(t)) \sin(kZ_0(t)) - \cos(kX_0(t)) \cos(kY_0(t)) \cos(kZ_0(t)) \Big) \right].$$

The constants A,B and C are determined by the initial values of the Navier-Stokes equation (1), and our model (3), so let us suppose that  $\max\{|A|,|B|,|C|\} < n$ . Furthermore, the range of functions  $\cos(kX_0(t))\sin(kY_0(t)) + \cos(kX_0(t))\sin(kX_0(t))\cos(kX_0(t))\sin(kX_0(t))\sin(kX_0(t))\cos$ 

$$Det(S(t)) > \frac{1}{\tau^3} \left[ (1 - \alpha + \tau)^3 - \frac{3}{2} k^2 (1 - \alpha + \tau) (1 - \alpha)^4 n^2 - k^3 (1 - \alpha)^6 n^3 \right].$$

Finally, since we know that parametar k is arbitrary in Trkal solution (2), then for any n > 0, we can choose k = k(n) small enough to ensure that Det(S(t)) > 0, which gives that S(t) is a regular matrix for any  $t \in [0, T]$ . Further, let us denote by  $P_{\alpha}$  the vector  $P_{\alpha}(t) = (U_{\alpha}(t), V_{\alpha}(t), W_{\alpha}(t), X_{\alpha}(t), Y_{\alpha}(t), Z_{\alpha}(t))^{T}$ ,  $\alpha \in I$ . In the sequel, we prove two auxiliary results, which will lead to the main theorem.

**Lemma 1.1.** The system of ODEs (8)-(9) has a unique solution  $P_0(t) \in C^1([0,T],[-L,L]^6)$ , and it is satisfied that

$$\sup_{t \in [0,T]} ||P_{\mathbf{0}}(t)||_{[-L,L]^{6}} \le ||P_{\mathbf{0}}^{0}|| + (2 - \alpha + \alpha T) \left[ 2 \left( |A| + |B| + |C| \right) \frac{3 - 3\alpha + \tau}{1 - \alpha + \tau} + ||\mathbf{U}_{\mathbf{0}}^{0}|| \right] e^{\frac{\alpha T}{1 - \alpha + \tau}}. \tag{16}$$

*Proof.* The system (8)-(9) after simple rearrangement, can be written in matrix form

$$S(t)P'_{0}(t) = F_{0}(t),$$
 (17)

where

$$F_{0}(t) = \begin{bmatrix} -\frac{\alpha}{\tau}U_{0}(t) + \left(\frac{1-\alpha}{\tau}(-\nu k^{2}) + \frac{\alpha}{\tau}\right)e^{-\nu k^{2}t}\left(A\sin(kZ_{0}(t)) + C\cos(kY_{0}(t))\right) \\ -\frac{\alpha}{\tau}V_{0}(t) + \left(\frac{1-\alpha}{\tau}(-\nu k^{2}) + \frac{\alpha}{\tau}\right)e^{-\nu k^{2}t}\left(B\sin(kX_{0}(t)) + A\cos(kZ_{0}(t))\right) \\ -\frac{\alpha}{\tau}W_{0}(t) + \left(\frac{1-\alpha}{\tau}(-\nu k^{2}) + \frac{\alpha}{\tau}\right)e^{-\nu k^{2}t}\left(C\sin(kY_{0}(t)) + B\cos(kX_{0}(t))\right) \\ \alpha U_{0}(t) \\ \alpha V_{0}(t) \\ \alpha W_{0}(t) \end{bmatrix}.$$

By taking into account that S(t) is a regular matrix for  $t \in [0, T]$ , we obtain

$$P_0'(t) = S^{-1}(t)F_0(t). (18)$$

By observing that all components of the matrix valued functions S(t) and  $F_0(t)$  are either constants or products of cosine, sine, and exponential functions, hence continuous w.r.t.  $t \in [0, T]$ , and clearly since  $S^{-1}(t)F_0(t)$  is Lipschitz continuous with respect to any component function of  $P_0(t)$ , we conclude by the Picard-Lindelöf theorem that there is a unique solution  $P_0(t)$  of system (8)-(9) and it belongs to  $C^1([0, T], [-L, L]^6)$ . In order to obtain the desired estimate (16) for the solution  $P_0(t)$  in the supremum norm, let us consider the first equation of system (8), which is given by

$$U_0'(t) = (1 - a) \frac{d}{dt} \left[ -\frac{1}{\tau} U_0(t) + \frac{1}{\tau} e^{-\nu k^2 t} \left( A \sin(kZ_0(t)) + C \cos(kY_0(t)) \right) \right]$$

$$+ a \left[ -\frac{1}{\tau} U_0(t) + \frac{1}{\tau} e^{-\nu k^2 t} \left( A \sin(kZ_0(t)) + C \cos(kY_0(t)) \right) \right].$$

After integration over the interval [0, t], and by using the initial values  $X_0(0) = (X_0^0, Y_0^0, Z_0^0)$  and  $U_0(0) = U_0^0$ , we arrive to

$$\begin{split} \left(1 + \frac{1 - \mathfrak{a}}{\tau}\right) \left(U_0(t) - U_0^0\right) &= \frac{1 - \mathfrak{a}}{\tau} \left(e^{-\nu k^2 t} \left(A \sin(kZ_0(t)) + C \cos(kY_0(t))\right) - A \sin(kZ_0^0) - C \cos(kY_0^0)\right) \\ &+ \frac{\mathfrak{a}}{\tau} \int_0^t \left(-U_0(s) + e^{-\nu k^2 s} \left(A \sin(kZ_0(s)) + C \cos(kY_0(s))\right)\right) ds, \end{split}$$

which by taking the absolute value of both sides and using the triangle inequality leads to

$$\begin{split} (1-\alpha+\tau)|U_0(t)| \leq & 2(1-\alpha)(|A|+|C|) + (1-\alpha+\tau)|U_0^0| + \alpha \int_0^t \left(|A|+|C|+|U_0(s)|\right) ds \\ & = 2(1-\alpha)(|A|+|C|) + (1-\alpha+\tau)|U_0^0| + \alpha(|A|+|C|)t + \alpha \int_0^t |U_0(s)| ds. \end{split}$$

After dividing by  $1 - a + \tau$ , we are able to apply Grönwall's inequality and obtain

$$\begin{split} |U_{0}(t)| &\leq 2\frac{1-\mathfrak{a}}{1-\mathfrak{a}+\tau}(|A|+|C|)+|U_{0}^{0}|+\frac{\mathfrak{a}}{1-\mathfrak{a}+\tau}(|A|+|C|)t\\ &+\frac{\mathfrak{a}}{1-\mathfrak{a}+\tau}\int_{0}^{t}\left(2\frac{1-\mathfrak{a}}{1-\mathfrak{a}+\tau}(|A|+|C|)+|U_{0}^{0}|+\frac{\mathfrak{a}}{1-\mathfrak{a}+\tau}(|A|+|C|)s\right)e^{\frac{\mathfrak{a}(t-s)}{1-\mathfrak{a}+\tau}}ds. \end{split}$$

By using integration by parts, we straightforwardly obtain

$$|U_0(t)| \le \left(2\frac{1-\mathfrak{a}}{1-\mathfrak{a}+\tau}(|A|+|C|)+|U_0^0|+|A|+|C|\right)e^{\frac{\mathfrak{a}t}{1-\mathfrak{a}+\tau}}-(|A|+|C|),$$

and since  $t \in [0, T]$ , it implies that

$$|U_0(t)| \leq \left(2\frac{1-\mathfrak{a}}{1-\mathfrak{a}+\tau}(|A|+|C|)+|U_0^0|+|A|+|C|\right)e^{\frac{aT}{1-\mathfrak{a}+\tau}} := \mathcal{K}(A,C,\mathfrak{a},\tau,T,U_0^0).$$

By following exactly the same approach, we obtain estimates for solutions  $V_0(t)$  and  $W_0(t)$ , i.e.

$$|V_0(t)| \le \mathcal{K}(B, A, \mathfrak{a}, \tau, T, V_0^0), \quad |W_0(t)| \le \mathcal{K}(C, B, \mathfrak{a}, \tau, T, W_0^0).$$

In the sequel we derive similar estimates for the solutions  $X_0(t)$ ,  $Y_0(t)$  and  $Z_0(t)$ . Firstly, let us focus on the equation of system (9) given by

$$X_0'(t) = (1 - a)U_0'(t) + aU_0(t).$$

After integration over the interval [0, t], and using initial values  $X_0(0) = X_0^0$ , and  $U_0(0) = U_0^0$ , we arrive to

$$X_{\mathbf{0}}(t) - X_{\mathbf{0}}^{0} = (1 - \mathfrak{a})(U_{\mathbf{0}}(t) - U_{\mathbf{0}}^{0}) + \mathfrak{a} \int_{0}^{t} U_{\mathbf{0}}(s)ds,$$

thus

$$|X_0(t)| \le |X_0^0| + (1-\mathfrak{a})|U_0^0| + (1-\mathfrak{a})|U_0(t)| + \mathfrak{a} \int_0^t |U_0(s)|ds.$$

By the previous inequality obtained for  $|U_0(t)|$ , we obtain

$$|X_0(t)| \le |X_0^0| + (1-\alpha)|U_0^0| + (1-\alpha+\alpha T)\mathcal{K}(A,C,\alpha,\tau,T,U_0).$$

Again, by following the same approach we derive that  $Y_0(t)$  and  $Z_0(t)$  are dominated by similar terms which correspond to estimates obtained for  $V_0(t)$  and  $W_0(t)$ , respectively, i.e. we know that

$$\begin{aligned} |Y_0(t)| &\leq |Y_0^0| + (1-\mathfrak{a})|V_0^0| + (1-\mathfrak{a}+\mathfrak{a}T)\mathcal{K}(B,A,\mathfrak{a},\tau,T,V_0), \\ |Z_0(t)| &\leq |Z_0^0| + (1-\mathfrak{a})|W_0^0| + (1-\mathfrak{a}+\mathfrak{a}T)\mathcal{K}(C,B,\mathfrak{a},\tau,T,W_0). \end{aligned}$$

Finally, after using the definition of norm  $\sup_{t \in [0,T]} \| \cdot \|_{[-L,L]^6}$ , inequality (16) follows directly.  $\square$ 

Before we formulate the next lemma, let us denote

$$f_{i,l}^n(t) = \mathbf{1}_{i,l} \frac{\sqrt{2\kappa_n}}{\Gamma(H+\frac{1}{2})} \int_0^t \frac{d}{ds} \int_{-\infty}^s \xi_j(\tau) (s-\tau)^{H-\frac{1}{2}} d\tau ds = \mathbf{1}_{i,l} \frac{\sqrt{2\kappa_n}}{\Gamma(H+\frac{1}{2})} \frac{A_j^H(t) - A_j^H(0)}{\sqrt{2^j j!} \sqrt{\pi}}.$$

where i = 3(j - 1) + l for  $j \in \mathbb{N}$ ,  $l \in \{0, 1, 2\}$ , and  $n \in \{1, 2\}$ .

**Lemma 1.2.** The system of ODEs (10)-(11) has a unique solution  $P_{\epsilon^{(i)}}(t) \in C^1([0,T],[-L,L]^6)$ , and it holds that

$$\sup_{t \in [0,T]} \|P_{\epsilon^{(i)}}(t)\|_{[-L,L]^6} \le \left( \|S(0)\| \|P_{\epsilon^{(i)}}^0\| + 8(\sqrt{\kappa_1} + \sqrt{\kappa_2})(1+T)MG^H(T) \right) \|S^{-1}\| e^{\|N\| \|S^{-1}\| T}, \tag{19}$$

where  $P_{\epsilon^{(i)}}^0 = P_{\epsilon^{(i)}}(0)$ , and the matrices N and  $S^{-1}$  are given as upper bounds of N(t) and  $S^{-1}(t)$ , i.e.  $|N(t)| \leq N$ , and  $|S^{-1}(t)| \leq S^{-1}$ , for  $t \in [0,T]$ , and the matrix inequalities are considered as explained in Appendix F.

*Proof.* Similarly as in the previous lemma, since we defined matrix valued functions S(t) and N(t), after integration over [0, t], our system becomes equivalent to

$$S(t)P_{\epsilon^{(i)}}(t) = S(0)P_{\epsilon^{(i)}}^{0} + F_{\epsilon^{(i)}}(t) + \int_{0}^{t} N(s)P_{\epsilon^{(i)}}(s)ds, \tag{20}$$

where

$$F_{\epsilon^{(i)}}(t) = (1 - \mathfrak{a}) f_{\epsilon^{(i)}}(t) + \mathfrak{a} \int_0^t f_{\epsilon^{(i)}}(s) ds,$$

for  $f_{\epsilon^{(i)}}(t) = (f_{i,1}^1(t), f_{i,2}^1(t), f_{i,0}^1(t), f_{i,2}^2(t), f_{i,2}^2(t), f_{i,2}^2(t))^T$ . Notice, for fixed  $i \in \mathbb{N}$  only two functions in the vector valued function  $f_{\epsilon^{(i)}}(t)$  survive, while the other four become equal to zero, depending on whether the remainder on division i by 3 is equal to 1, 2 or 0. By using (F.1), we differentiate equation (20) with respect to t, and get

$$S'(t)P_{\epsilon^{(i)}}(t) + S(t)P'_{\epsilon^{(i)}}(t) = F'_{\epsilon^{(i)}}(t) + N(t)P_{\epsilon^{(i)}}(t).$$

Since the matrix S(t) is regular for any  $t \in [0, T]$ , we can multiply the above equation by  $S^{-1}(t)$ , and obtain

$$P'_{\epsilon^{(i)}}(t) = S^{-1}(t) \left( F'_{\epsilon^{(i)}}(t) + (N(t) - S'(t)) P_{\epsilon^{(i)}}(t) \right).$$

Clearly, the matrix valued functions  $S^{-1}(t)$ , S'(t), and N(t) are continuous in t on [0,T]. The vector valued function  $F'_{\epsilon^{(i)}}(t)$  contains functions  $\frac{d}{dt}f^n_{i,l'}$ , which are up to a constant equal to  $\frac{d}{dt}A^H_j(t)$ , which are by (A.5) and (A.6) continuous in t on the interval [0,T]. Moreover, Lipschitz continuity in  $P_{\epsilon^{(i)}}$  is satisfied, thus according to the Picard-Lindelöf theorem there is a unique solution of system (10)-(11) on [0,T]. Furthermore, let us multiply by  $S^{-1}(t)$  equation (20), to obtain

$$P_{\epsilon^{(i)}}(t) = S^{-1}(t)S(0)P_{\epsilon^{(i)}}^0 + S^{-1}(t)F_{\epsilon^{(i)}}(t) + S^{-1}(t)\int_0^t N(s)P_{\epsilon^{(i)}}(s)ds,$$

which implies

$$|P_{\epsilon^{(i)}}(t)| \leq |S^{-1}(t)||S(0)||P_{\epsilon^{(i)}}^{0}| + |S^{-1}(t)||F_{\epsilon^{(i)}}(t)| + |S^{-1}(t)| \int_{0}^{t} |N(s)||P_{\epsilon^{(i)}}(s)|ds.$$

Since the components of  $S^{-1}(t)$  and N(t) are continuous functions over [0, T], there exist matrices  $S^{-1}$  and N such that  $|S_1^{-1}(t)| \le S_1^{-1}$ ,  $N(t) \le N$  for  $t \in [0, T]$ , which imply the inequality

$$|P_{\epsilon^{(i)}}(t)| \le S^{-1}|S(0)||P_{\epsilon^{(i)}}^0| + S^{-1}|F_{\epsilon^{(i)}}(t)| + S^{-1} \int_0^t N|P_{\epsilon^{(i)}}(s)|ds,$$

so by using Grönwall's inequality Theorem F.1, one gets

$$|P_{\epsilon^{(i)}}(t)| \leq S^{-1}\left(|S(0)||P_{\epsilon^{(i)}}^{0}| + |F_{\epsilon^{(i)}}(t)|\right) + S^{-1}\int_{0}^{t} e^{NS^{-1}(t-s)}NS^{-1}\left(|S(0)||P_{\epsilon^{(i)}}^{0}| + |F_{\epsilon^{(i)}}(s)|\right)ds.$$

Hence, by taking the norm  $\sup_{t \in [0,T]} \| \cdot \|_{[-L,L]^6}$  on both sides, we arrive to

$$\begin{split} \sup_{t \in [0,T]} & \| P_{\epsilon^{(i)}}(t) \|_{[-L,L]^6} \leq \| S^{-1} \| \left( \| S(0) \| \| P_{\epsilon^{(i)}}^0 \| + \sup_{t \in [0,T]} \| F_{\epsilon^{(i)}}(t) \|_{[-L,L]^6} \right) \\ & + \| S^{-1} \| \int_0^t e^{\| N \| \| S^{-1} \| (t-s)} \| N \| \| S^{-1} \| \left( \| S(0) \| \| P_{\epsilon^{(i)}}^0 \| + \sup_{s \in [0,t]} \| F_{\epsilon^{(i)}}(s) \|_{[-L,L]^6} \right) ds \\ & \leq \| S^{-1} \| \left( \| S(0) \| \| P_{\epsilon^{(i)}}^0 \| + \sup_{t \in [0,T]} \| F_{\epsilon^{(i)}}(t) \|_{[-L,L]^6} \right) \left( 1 + \int_0^t e^{\| N \| \| S^{-1} \| (t-s)} \| N \| \| S^{-1} \| ds \right). \end{split}$$

Note that by Lemma A.3, it follows that  $\frac{|A_j^H(t)-A_j^H(0)|}{\sqrt{2^j j!} \sqrt{\pi}} \le 4MG^H(t)$ , and for  $H \in (0,1)$ ,  $j \in \mathbb{N}$  we have

$$|f_{i,l}^n(t)| \leq \mathbf{1}_{i,l} \frac{\sqrt{2\kappa_n}}{\Gamma(H+\frac{1}{2})} \frac{|A_j^H(t) - A_j^H(0)|}{\sqrt{2^j j! \sqrt{\pi}}} \leq \mathbf{1}_{i,l} \frac{\sqrt{2\kappa_n}}{\Gamma(H+\frac{1}{2})} 4MG^H(T) \leq \frac{4\sqrt{2}}{\Gamma(H+\frac{1}{2})} \sqrt{\kappa_n} MG^H(T),$$

thus since  $a \in [0,1]$  and  $\frac{4\sqrt{2}}{\Gamma(H+\frac{1}{2})} < 8$  for  $H \in (0,1)$ , one gets

$$\sup_{t \in [0,T]} ||F_{\epsilon^{(t)}}(s)||_{[-L,L]^6} \le (1-\mathfrak{a})(\sqrt{\kappa_1} + \sqrt{\kappa_2})8MG^H(T) + \mathfrak{a}T(\sqrt{\kappa_1} + \sqrt{\kappa_2})8MG^H(T)$$

$$\le 8(\sqrt{\kappa_1} + \sqrt{\kappa_2})(1+T)MG^H(T).$$

Finally, by using this estimate and simple integration one obtains (19), for  $t \in [0, T]$ .  $\square$ 

**Lemma 1.3.** The system of ODEs (12)-(13) has a unique solution  $P_{\alpha}(t) \in C^1([0,T],[-L,L]^6)$  where  $|\alpha| > 1$ , and for  $L_{\alpha} = \sup_{t \in [0,T]} ||P_{\alpha}(t)||_{[-L,L]^6}$ , and  $P_{\alpha}^0 = P_{\alpha}(0)$ , it is satisfied that

$$L_{\alpha} \leq ||S(0)|||P_{\alpha}^{0}|||S^{-1}||e^{||N||||S^{-1}||T}$$

$$+ \frac{2}{\tau}(1+T)\max\{|A|,|B|,|C|\}||S^{-1}||e^{||N||||S^{-1}||T}$$

$$\times \sum_{n=2}^{|\alpha|} \frac{k^{n}}{n!} \sum_{0 < \gamma_{1} < \alpha} \sum_{0 < \gamma_{2} < \gamma_{1}} \cdots \sum_{0 < \gamma_{n-1} < \gamma_{n-2}} L_{\alpha-\gamma_{1}} L_{\gamma_{1}-\gamma_{2}} \dots L_{\gamma_{n-2}-\gamma_{n-1}} L_{\gamma_{n-1}},$$

$$(21)$$

*Proof.* In the two previous lemmas we proved uniqueness of a solution for the systems obtained for  $\alpha = \mathbf{0}$  and  $\alpha = \epsilon^{(i)}$ ,  $i \in \mathbb{N}$ . We proceed now by induction on the multiindex  $\alpha$ . Let us suppose that there is a unique solution of system (12)-(13) for every  $\beta \in \mathcal{I}$ ,  $\epsilon^{(i)} < \beta < \alpha$ . Then, for fixed  $|\alpha| > 1$  our system after integration over [0,t] becomes equal to

$$S(t)P_{\alpha}(t) = S(0)P_{\alpha}^{0} + F_{\alpha}(t) + \int_{0}^{t} N(s)P_{\alpha}(s)ds, \tag{22}$$

where

$$F_{\alpha}(t) = (1 - \mathfrak{a})f_{\alpha}(t) + \mathfrak{a} \int_{0}^{t} f_{\alpha}(s)ds,$$

for

$$f_{\alpha}(t) = \frac{1}{\tau} e^{-\nu k^2 t} \left( (Ar_{\alpha, \sin(kZ)}(t), Br_{\alpha, \sin(kX)}(t), Cr_{\alpha, \sin(kY)}(t), 0, 0, 0)^T + (Cr_{\alpha, \cos(kY)}(t), Ar_{\alpha, \cos(kZ)}(t), Br_{\alpha, \cos(kX)}(t), 0, 0, 0) \right)^T.$$

By (D.2), the functions  $r_{\alpha,\sin(\cdot)}$  and  $r_{\alpha,\cos(\cdot)}$  involve only solutions  $X_{\beta}$ ,  $Y_{\beta}$ ,  $Z_{\beta}$ , for lesser multiindexes  $\beta < \alpha$ , and they all belong to  $C^1([0,T],[-L,L])$  by assumption. Hence, after differentiating and then multiplying the obtained equation by  $S^{-1}(t)$  one arrives to

$$P'_{\alpha}(t) = S^{-1}(t) \left( F'_{\alpha}(t) + (N(t) - S'(t)P_{\alpha}(t)) \right)$$

from which it follows by the standard Picard-Lindelöf argument that there exists a unique solution of system (12)-(13), which belongs to  $C^1([0,T],[-L,L]^6)$ . Now, let us return to (22), which we multiply by  $S^{-1}(t)$  to obtain

$$P_{\alpha}(t) = S^{-1}(t)S(0)P_{\alpha}^{0} + S^{-1}(t)F_{\alpha}(t) + S^{-1}(t)\int_{0}^{t} N(s)P_{\alpha}(s)ds,$$

i.e.,

$$|P_{\alpha}(t)| \leq |S^{-1}(t)||S(0)||P_{\alpha}^{0}| + |S^{-1}(t)||F_{\alpha}(t)| + |S^{-1}(t)| \int_{0}^{t} |N(s)||P_{\alpha}(s)|ds.$$

Again, for the same matrices  $S^{-1}$  and N as in the previous lemma, we arrive to

$$|P_{\alpha}(t)| \leq S^{-1}|S(0)||P_{\alpha}^{0}| + S^{-1}|F_{\alpha}(t)| + S^{-1}\int_{0}^{t} N|P_{\alpha}(s)|ds,$$

so once more, Grönwall's inequality Theorem F.1 gives that

$$|P_{\alpha}(t)| \leq S^{-1} \left( |S(0)||P_{\alpha}^{0}| + |F_{\alpha}(t)| \right) + S^{-1} \int_{0}^{t} e^{NS^{-1}(t-s)} NS^{-1} \left( |S(0)||P_{\alpha}^{0}| + |F_{\alpha}(t)| \right) ds.$$

Taking the norm  $\sup_{t \in [0,T]} \| \cdot \|_{[-L,L]^6}$ , one obtains

$$L_{\alpha} \leq \|S^{-1}\| \left( \|S(0)\| \|P_{\alpha}^{0}\| + \sup_{t \in [0,T]} \|F_{\alpha}(t)\|_{[-L,L]^{6}} \right)$$

$$+ \|S^{-1}\| \int_{0}^{t} e^{\|N\|\|S^{-1}\|(t-s)} \|N\|\|S^{-1}\| \left( \|S(0)\| \|P_{\alpha}^{0}\| + \sup_{s \in [0,t]} \|F_{\alpha}(s)\|_{[-L,L]^{6}} \right) ds$$

$$\leq \|S^{-1}\| \left( \|S(0)\| \|P_{\alpha}^{0}\| + \sup_{t \in [0,T]} \|F_{\alpha}(t)\|_{[-L,L]^{6}} \right) \left( 1 + \int_{0}^{t} e^{\|N\|\|S^{-1}\|(t-s)} \|N\| \|S^{-1}\| ds \right).$$

$$(23)$$

Before we continue, let us recall the definition of  $r_{\alpha,\sin(\cdot)}(t)$  and  $r_{\alpha,\cos(\cdot)}(t)$ . In particular for  $X \in [-L,L] \otimes (FS)'$ , by (D.2), we have

$$r_{\alpha,\sin(kX)}(t) = \sum_{n=2}^{|\alpha|} \frac{k^n \sin\left(n\frac{\pi}{2} + kX_0\right)}{n!} \sum_{\mathbf{0} < \gamma_1 < \alpha} \sum_{\mathbf{0} < \gamma_2 < \gamma_1} \cdots \sum_{\mathbf{0} < \gamma_{n-1} < \gamma_{n-2}} X_{\alpha - \gamma_1}(t) X_{\gamma_1 - \gamma_2}(t) \dots X_{\gamma_{n-2} - \gamma_{n-1}}(t) X_{\gamma_{n-1}}(t),$$

$$r_{\alpha,\cos(kX)}(t) = \sum_{n=2}^{|\alpha|} \frac{k^n \cos\left(n\frac{\pi}{2} + kX_0\right)}{n!} \sum_{\mathbf{0} < \gamma_1 < \alpha} \sum_{\mathbf{0} < \gamma_2 < \gamma_1} \cdots \sum_{\mathbf{0} < \gamma_{n-1} < \gamma_{n-2}} X_{\alpha - \gamma_1}(t) X_{\gamma_1 - \gamma_2}(t) \dots X_{\gamma_{n-2} - \gamma_{n-1}}(t) X_{\gamma_{n-1}}(t).$$

Hence, by applying these formulas for the processes  $Y, Z \in [-L, L] \otimes (FS)'$ , and denoting  $L^x_\alpha = \sup_{t \in [0,T]} \|X_\alpha(t)\|_{[-L,L]}$ ,  $L^z_\alpha = \sup_{t \in [0,T]} \|Z_\alpha\|_{[-L,L]}$ , one obtains

$$\begin{split} \sup_{t \in [0,T]} ||F_{\alpha}(t)||_{[-L,L]^6} &\leq \frac{1}{\tau} \left( (1-\mathfrak{a}) \sup_{t \in [0,T]} ||f_{\alpha}(t)||_{[-L,L]^6} + \mathfrak{a} T \sup_{t \in [0,T]} ||f_{\alpha}(t)||_{[-L,L]^6} \right) \\ &\leq 2 \frac{1+T}{\tau} \max\{|A|,|B|,|C|\} \sum_{n=2}^{|\alpha|} \frac{k^n}{n!} \sum_{0 < \gamma_1 < \alpha} \sum_{0 < \gamma_2 < \gamma_1} \cdots \sum_{0 < \gamma_{n-1} < \gamma_{n-2}} \left( L^x_{\alpha - \gamma_1} L^x_{\gamma_1 - \gamma_2} \dots L^x_{\gamma_{n-2} - \gamma_{n-1}} L^x_{\gamma_{n-1}} + L^x_{\alpha - \gamma_1} L^x_{\gamma_1 - \gamma_2} \dots L^x_{\gamma_{n-2} - \gamma_{n-1}} L^x_{\gamma_{n-1}} \right) \\ &+ L^y_{\alpha - \gamma_1} L^y_{\gamma_1 - \gamma_2} \dots L^y_{\gamma_{n-2} - \gamma_{n-1}} L^y_{\gamma_{n-1}} + L^x_{\alpha - \gamma_1} L^x_{\gamma_1 - \gamma_2} \dots L^x_{\gamma_{n-2} - \gamma_{n-1}} L^x_{\gamma_{n-1}} \right) \\ &\leq 2 \frac{1+T}{\tau} \max\{|A|,|B|,|C|\} \sum_{n=2}^{|\alpha|} \frac{k^n}{n!} \sum_{0 < \gamma_1 < \alpha} \sum_{0 < \gamma_2 < \gamma_1} \cdots \sum_{0 < \gamma_{n-1} < \gamma_{n-2}} L_{\alpha - \gamma_1} L_{\gamma_1 - \gamma_2} \dots L_{\gamma_{n-2} - \gamma_{n-1}} L_{\gamma_{n-1}}. \end{split}$$

Finally, by combining this estimate and (23), one obtains (21).  $\square$ 

**Theorem 1.4.** There exists a unique solution  $P(t,\omega) \in C([0,T],[-L,L]^6) \otimes (FS)'$  to the stochastic fractional model system (3), where  $P(t,\omega) = (\mathbf{U}(t,\omega),\mathbf{X}(t,\omega))$ . Moreover, the expected value of this solution is  $E(P(t,\omega)) = P_0(t)$  given in Lemma 1.1.

*Proof.* According to Lemma 1.1, Lemma 1.2, and Lemma 1.3, for every  $\alpha > \mathbf{0}$  the system of corresponding ODEs has a unique solution  $P_{\alpha} \in C^1([0,T],[-L,L]^6)$ . Thus, the expansion  $P(t,\omega) = \sum_{\alpha \in I} P_{\alpha}(t)H_{\alpha}(\omega), t \in [0,T]$ ,

 $\omega \in \Omega$  has coefficients that are all unique solutions to the system of ODE obtained for corresponding  $\alpha$ . The uniqueness of our solution  $P(t,\omega)$  will follow from the uniqueness of the coordinatewise solutions  $P_{\alpha}$ ,  $\alpha \in I$ , and due to uniqueness of the Wiener-Itô chaos expansion of stochastic processes. Moreover, after we show that this expansion  $P(t,\omega)$  is convergent, its continuity follows directly from the continuity of the coefficients  $P_{\alpha}$ .

In Lemma 1.3 we derived a recurrent formula for  $L_{\alpha} = \sup_{t \in [0,T]} ||P_{\alpha}||_{[-L,L]^6}, |\alpha| > 1$ . Now, we prove that  $P(t,\omega) \in C([0,T],[-L,L]^6) \otimes (FS)'$ .

Let  $P^0(\omega) := P(0,\omega) \in [-L,L]^6 \otimes (FS)'$  be an initial condition, hence there exist  $\widetilde{r} \ge 2$  and  $\widetilde{p} > g$  such that  $\sum_{\alpha \in \mathcal{I}} \|P^0_\alpha\|^2 \alpha!^2 (\overline{r}^{[\alpha]^3}!)^{-2} (2\mathbb{N})^{-2\overline{p}\alpha} = K^2$  for some  $K \ge 0$ . Equivalently,

$$(\exists \widetilde{r} \ge 2)(\exists \widetilde{p} > q)(\exists K \ge 0)(\forall \alpha \in I) \quad ||P_{\alpha}^{0}|| \le K\alpha! \widehat{r}^{|\alpha|^{3}}! (2\mathbb{N})^{\widetilde{p}\alpha}, \tag{24}$$

where g > 1 is chosen so that  $B^H(t) \in S'(\mathbb{R}) \otimes S_{-1,-g}$  as stated in (C.5). As the first step we give an upper bound for  $L_{\alpha}$ ,  $|\alpha| > 0$ , i.e. we prove that there exist  $r \ge 2$  and  $p \ge \widetilde{p}$  such that

$$L_{\alpha} \le \alpha! (2\mathbb{N})^{p\alpha} r^{|\alpha|^3}!, \quad |\alpha| > 0, \ \alpha \in \mathcal{I}, \tag{25}$$

where  $r > r_0$  for

$$r_0 := 2\left(\widetilde{r} + \|S^{-1}\|e^{\|N\|\|S^{-1}\|T}\left(\|S(0)\|K + \frac{1+T}{\tau}D\max\{|A|, |B|, |C|\} + 4(\sqrt{\kappa_1} + \sqrt{\kappa_2})(1+T)MG^H(T)\right)\right), \quad (26)$$

and D > 0. In [26] it was proved that for  $\alpha \in I \setminus \mathbf{0}$  and given  $k \in \mathbb{N}$ ,  $k \le |\alpha|$ , the number  $N(\alpha, k)$  of all possible combinations in which a multiindex  $\alpha$  can be written as a sum of k strictly smaller and nonzero multiindeces is less then or equal to  $2^{k|\alpha|}$ .

Firstly, for  $|\alpha| = 1$  one directly obtains from (19) and (24) that (25) is satisfied.

Secondly, let us examine the case  $|\alpha| = 2$ . Denote by  $J_2 = \sum_{0 < \gamma_1 < \alpha} L_{\alpha - \gamma_1} L_{\gamma_1}$ , and note that

$$L_{\alpha} \leq \left( ||S(0)|| ||P_{\alpha}^{0}|| + 2\frac{1+T}{\tau} \max\{|A|, |B|, |C|\} \frac{k^{2}}{2!} J_{2} \right) ||S^{-1}|| e^{||N|| ||S^{-1}|| T}.$$

Notice, for any  $k \in \mathbb{R}$ , there exists D > 0 such that  $\frac{k^n}{n!} < D^n$ , for any  $n \ge 2$ . The sum  $J_2$  over  $\gamma_1 \in I$ ,  $0 < \gamma_1 < \alpha$  has  $N(\alpha, 2) \le 2^{2|\alpha|} = 2^4$  terms, and since  $|\alpha - \gamma_1| = 1$ ,  $|\gamma_1| = 1$ , by using the estimate for  $|\alpha| = 1$ , and the estimate for the initial condition, one has

$$\begin{split} L_{\alpha} &\leq \|S(0)\| \|S^{-1}\| e^{\|N\|\|S^{-1}\|T} K\alpha ! \vec{r}^{|\alpha|^{3}} ! (2\mathbb{N})^{\widetilde{p}\alpha} \\ &+ 2\frac{1+T}{\tau} \max\{|A|,|B|,|C|\} \|S^{-1}\| e^{\|N\|\|S^{-1}\|T} \widetilde{D}^{|\alpha|} (\alpha-\gamma_{1}) ! (2\mathbb{N})^{(\alpha-\gamma_{1})p} r^{|\alpha-\gamma_{1}|^{3}} ! (\gamma_{1}) ! (2\mathbb{N})^{\gamma_{1}p} r^{|\gamma_{1}|^{3}} !, \end{split}$$

where  $\widetilde{D}=(2D)^2$ . Hence, by  $(\alpha-\gamma_1)!\gamma_1!\leq \alpha!$ ,  $p\geq \widetilde{p}$  this implies

$$L_{\alpha} \leq \left( ||S(0)||Kr^{|\alpha|^3}! + 2\frac{1+T}{\tau} \max\{|A|, |B|, |C|\}\widetilde{D}^{|\alpha|}r!r! \right) ||S^{-1}||e^{||N||||S^{-1}||T} \alpha! (2\mathbb{N})^{p\alpha}.$$

By using  $(r!)^n \le (r^n)!$  for  $n \in \mathbb{N}$ , and  $r > r_0$  one obtains

$$L_{\alpha} \le \alpha! (2\mathbb{N})^{p\alpha} r^8!. \tag{27}$$

Now, we suppose that (25) is satisfied for  $0 < |\alpha| \le m$ , where  $m \in \mathbb{N}$ . It remains to prove the same for  $|\alpha| = m + 1$ . Let us denote by

$$J_n = \sum_{\mathbf{0} < \gamma_1 < \alpha} \sum_{\mathbf{0} < \gamma_2 < \gamma_1} \cdots \sum_{\mathbf{0} < \gamma_{n-1} < \gamma_{n-2}} L_{\alpha - \gamma_1} L_{\gamma_1 - \gamma_2} \dots L_{\gamma_{n-2} - \gamma_{n-1}} L_{\gamma_{n-1}}. \tag{28}$$

Notice that  $J_n$  has less than or equal to  $2^{n|\alpha|}$  terms, and  $1 \le |\alpha - \gamma_1|, |\gamma_1 - \gamma_2|, \dots, |\gamma_{n-2} - \gamma_{n-1}|, |\gamma_{n-1}| \le m$ . From the inductive hypothesis and fact that  $(\alpha - \gamma_1)!(\gamma_1 - \gamma_2)! \cdots (\gamma_{n-2} - \gamma_{n-1})!\gamma_{n-1}! \le \alpha!$ , one gets

$$\begin{split} J_n &\leq 2^{n|\alpha|} \alpha! (2\mathbb{N})^{p(\alpha-\gamma_1)} r^{|\alpha-\gamma_1|^3}! (2\mathbb{N})^{p(\gamma_1-\gamma_2)} r^{|\gamma_1-\gamma_2|^3}! \dots (2\mathbb{N})^{p(\gamma_{n-2}-\gamma_{n-1})} r^{|\gamma_{n-1}-\gamma_{n-2}|^3}! (2\mathbb{N})^{p\gamma_{n-1}} r^{|\gamma_{n-1}|^3}! \\ &\leq 2^{n|\alpha|} \alpha! (2\mathbb{N})^{p\alpha} r^{|\alpha-\gamma_1|^3}! r^{|\gamma_1-\gamma_2|^3}! \dots r^{|\gamma_{n-1}-\gamma_{n-2}|^3}! r^{|\gamma_{n-1}|^3}!. \end{split}$$

Note that for r > 2 and positive numbers a and b it holds that  $r^{a^3}!r^{b^3}! \le (r^{a^3} + r^{b^3})! \le r^{a^3+b^3}! \le r^{(a+b)^3}!$ , thus for  $|\alpha - \gamma_1|, |\gamma_1 - \gamma_1| > 0$  it follows that  $r^{|\alpha - \gamma_1|^3}!r^{|\gamma_1 - \gamma_2|^3}! \le r^{|\alpha - \gamma_2|^3}!$ , so one concludes that

$$r^{|\alpha-\gamma_1|^3}!r^{|\gamma_1-\gamma_2|^3}!\dots r^{|\gamma_{n-1}-\gamma_{n-2}|^3}!r^{|\gamma_{n-1}|^3}! \leq r^{|\alpha-\gamma_{n-1}|^3+|\gamma_{n-1}|^3}!.$$

Moreover, for  $\beta \in \mathcal{I}$  it holds that  $(|\alpha| - |\beta|)^3 + |\beta|^3 \le (|\alpha| - 1)^3 + 1$ , where  $\beta < \alpha$ ,  $|\beta| \ge 1$ , so one obtains

$$r^{|\alpha-\gamma_1|^3}!r^{|\gamma_1-\gamma_2|^3}!\dots r^{|\gamma_{n-1}-\gamma_{n-2}|^3}!r^{|\gamma_{n-1}|^3}! < r^{(|\alpha|-1)^3+1}!.$$

Hence, we obtain that

$$J_n \le 2^{n\alpha} \alpha! (2\mathbb{N})^{p\alpha} r^{(|\alpha|-1)^3+1}!, \quad n = 2, \dots, |\alpha|. \tag{29}$$

Now, by using this estimate, one has that

$$\begin{split} L_{\alpha} &\leq \left( \|S(0)\| \|P_{\alpha}^{0}\| + 2\frac{1+T}{\tau} \max\{|A|, |B|, |C|\} \sum_{n=2}^{|\alpha|} \frac{k^{n}}{n!} J_{n} \right) \|S^{-1}\| e^{\|N\| \|S^{-1}\| T} \\ &\leq \|S(0)\| \|S^{-1}\| e^{\|N\| \|S^{-1}\| T} K_{\alpha} \widehat{r}^{|\alpha|^{3}} ! (2\mathbb{IN})^{\widetilde{p}\alpha} \\ &+ 2\frac{1+T}{\tau} \max\{|A|, |B|, |C|\} \|S^{-1}\| e^{\|N\| \|S^{-1}\| T} \sum_{n=2}^{|\alpha|} \frac{k^{n}}{n!} 2^{n|\alpha|} \alpha ! (2\mathbb{IN})^{p\alpha} r^{(|\alpha|-1)^{3}+1} !, \end{split}$$

and since

$$\sum_{n=2}^{|\alpha|} \frac{k^n}{n!} 2^{n|\alpha|} \le \sum_{n=2}^{|\alpha|} D^n 2^{n|\alpha|} = \sum_{n=2}^{|\alpha|} (D2^{|\alpha|})^n \le (D2^{|\alpha|})^{|\alpha|+1} \le (2D)^{|\alpha|^2 + |\alpha|} \le \widetilde{D}^{|\alpha|^2},$$

and once more  $p \ge \widetilde{p}$  and  $r > r_0$ , it follows that

$$\begin{split} L_{\alpha} &\leq \|S(0)\| \|S^{-1}\| e^{\|N\| \|S^{-1}\| T} K \alpha! \widetilde{r}^{|\alpha|^{3}}! (2\mathbb{N})^{\widetilde{p}\alpha} + 2\frac{1+T}{\tau} \max\{|A|,|B|,|C|\} \|S^{-1}\| e^{\|N\| \|S^{-1}\| T} \widetilde{D}^{|\alpha|^{2}} \alpha! (2\mathbb{N})^{p\alpha} r^{(|\alpha|-1)^{3}+1}! \\ &\leq \alpha! (2\mathbb{N})^{p\alpha} \|S^{-1}\| e^{\|N\| \|S^{-1}\| T} \left( \|S(0)\| K \widetilde{r}^{|\alpha|^{3}}! + 2\frac{1+T}{\tau} \max\{|A|,|B|,|C|\} \widetilde{D}^{|\alpha|^{2}} r^{(|\alpha|-1)^{3}+1} \right) \\ &\leq \alpha! (2\mathbb{N})^{p\alpha} r^{(m+1)^{3}}!. \end{split}$$

In the second step it is left to show that  $P(t,\omega) \in C([0,T],[-L,L]^6) \otimes (FS)'$ , i.e. that there exist  $s \ge 2$  and  $q \ge 0$  such that  $P(t,\omega) \in C([0,T],[-L,L]^6) \otimes (FS)_{-s,-q}$ . Indeed, we show that for  $P(t,\omega) = \sum_{\alpha \in \mathcal{I}} P_\alpha(t) H_\alpha(\omega)$  there exist  $s \ge 2$  and  $q \ge 0$  such that

$$\sum_{\alpha \in I} \sup_{t \in [0,T]} \|P_{\alpha}(t)\|_{[-L,L]^6}^2 \alpha! (s^{|\alpha|^3}!)^{-1} (2\mathbb{N})^{-q\alpha} = \sum_{\alpha \in I} L_{\alpha}^2 \alpha! (s^{|\alpha|^3}!)^{-1} (2\mathbb{N})^{-q\alpha} < \infty.$$
(30)

For all  $\alpha \in \mathcal{I}$ ,  $|\alpha| > 0$  by (25) it holds that

$$L_{\alpha}^{2} \leq (\alpha !)^{2} (2\mathbb{N})^{2p\alpha} (r^{|\alpha|^{3}}!)^{2} \leq (\alpha !)^{2} (2\mathbb{N})^{2p\alpha} r^{2|\alpha|^{3}}!.$$

Moreover, since  $\alpha! \leq r^{|\alpha|^3}!$ , then for all  $\alpha \in \mathcal{I}$ ,  $|\alpha| > 0$  follows that

$$L_{\alpha}^2 \leq (2\mathbb{N})^{2p\alpha} r^{4|\alpha|^3}!.$$

Finally, if we once more use that  $\alpha! \le r^{|\alpha|^3}!$ , and then choose  $s = r^5$  and q > 2p + 1, we arrive to

$$\begin{split} \sum_{\alpha \in I} L_{\alpha}^{2} \alpha! (s^{|\alpha|^{3}}!)^{-1} (2\mathbb{N})^{-q\alpha} &\leq L_{0}^{2} + \sum_{\alpha \in I \setminus \mathbf{0}} (2\mathbb{N})^{2p\alpha} r^{5|\alpha|^{3}}! (r^{5|\alpha|^{3}}!)^{-1} (2\mathbb{N})^{-q\alpha} \\ &\leq L_{0}^{2} + \sum_{\alpha \in I \setminus \mathbf{0}} (2\mathbb{N})^{(2p-q)\alpha} < \infty. \end{split}$$

Since the zeroth coefficient in the Wiener-Itô chaos expansion equals to the expectation of a stochastic process, it follows that the function  $P_0(t)$  from Lemma 1.1 has an important interpretation itself, namely it corresponds to the expectation of the solution to (3).

## 2. Numerical experiments and simulations

In this section we provide some simulations of the expiratory event and aerosol diffusion by using the proposed model (3) with Caputo-Fabrizio derivatives for a vanishing temporal lag in the Navier-Stokes airflow and fractional Brownian motion as a chaotic source term.

## 2.1. Numerical estimates of truncation errors

Before we turn to the simulation part, we provide results related to norm error estimation of two types of truncated chaos expansions. Let Index( $\alpha$ ) = max{j,  $\alpha_j \neq 0$ } for  $\alpha \in \mathcal{I}$  and consider the truncated chaos expansion of the solution  $P(t, \omega)$  as  $P_N(t, \omega) = \sum_{\text{Index}(\alpha) \leq N} P_\alpha(t) H_\alpha(\omega)$ .

**Theorem 2.1.** Let  $N \in \mathbb{N}_0$ , then the norm error estimate of the truncated chaos expansion  $P_N(t, \omega)$  can be expressed as

$$||P(t,\omega) - P_N(t,\omega)||^2_{C([0,T],[-L,L]^6)\otimes(FS)_{-s,-q}} \le \frac{\pi}{2q-2p+1}\zeta(q-2p,N+1), \quad s \ge r^5, \ q > 2p+2, \tag{31}$$

where r and p are chosen so that (25) is satisfied, while  $\zeta(\cdot,\cdot)$  represents the Hurwitz zeta function defined by

$$\zeta(a,b) = \sum_{n=0}^{\infty} \frac{1}{(n+b)^a}, \quad a > 1, \quad b \neq -1, -2, -3, \dots$$

*Proof.* By using the same notation as in the proof of Theorem 1.4, we obtain that

$$\begin{split} \|P(t,\omega) - P_N(t,\omega)\|_{C([0,T],[-L,L]^6)\otimes(FS)_{-s,-q}}^2 &= \|\sum_{\mathrm{Index}(\alpha)>N} P_\alpha(t) H_\alpha(\omega)\|_{C([0,T],[-L,L]^6)\otimes(FS)_{-s,-q}}^2 \\ &= \sum_{\mathrm{Index}(\alpha)>N} L_\alpha^2 \alpha! (s^{|\alpha|^3}!)^{-1} (2\mathbb{IN})^{-q\alpha} \\ &\leq \sum_{\mathrm{Index}(\alpha)>N} (2\mathbb{IN})^{(2p-q)\alpha}. \end{split}$$

Taking into account the ideas given in [21] and [54], we can rewrite the obtained sum as

$$\begin{split} \sum_{\mathrm{Index}(\alpha)>N} (2\mathbb{N})^{(2p-q)\alpha} &= \sum_{n=N+1}^{+\infty} \sum_{\substack{\alpha \\ \mathrm{Index}(\alpha)=n}} (2\mathbb{N})^{(2p-q)\alpha} \\ &= \sum_{n=N+1}^{\infty} \sum_{\substack{\alpha_1,\alpha_2,\dots,\alpha_{n-1}\geq 0 \\ \alpha_n\geq 1}} \prod_{j=1}^{n} (2j)^{(2p-q)\alpha_j} \\ &= \sum_{n=N+1}^{\infty} \left[ \prod_{j=1}^{n-1} \left( \sum_{\alpha_j=0}^{\infty} (2j)^{(2p-q)\alpha_j} \right) \right] \left( \sum_{\alpha_n=1}^{\infty} (2n)^{(2p-q)\alpha_n} \right) \end{split}$$

$$= \sum_{n=N+1}^{\infty} \frac{1}{(2n)^{q-2p}} \prod_{j=1}^n \frac{(2j)^{q-2p}}{(2j)^{q-2p}-1}.$$

It is straightforward to check that the sequence  $l_n(q-2p):=\prod_{j=1}^n\frac{(2j)^{q-2p}}{(2j)^{q-2p}-1}$  is monotonically increasing and convergent for any q>2p+1, and that  $\lim_{n\to\infty}l_n(2)=\lim_{n\to\infty}\prod_{j=1}^n\frac{(2j)^2}{(2j)^2-1}=\frac{\pi}{2}$ . Consequently, we see that  $l_n(q-2p)\leq l_n(2)$  so  $\lim_{n\to\infty}l_n(q-2p)\leq \frac{\pi}{2}$ , for any q>2p+2. Finally by applying this inequality, we arrive to

$$||P(t,\omega) - P_N(t,\omega)||^2_{C([0,T],[-L,L]^6)\otimes (FS)_{-s,-q}} \leq \sum_{n=N+1}^{\infty} \frac{1}{(2n)^{q-2p}} l_n(q-2p) \leq \frac{\pi}{2} \sum_{n=N+1}^{\infty} \frac{1}{(2n)^{q-2p}} l_n(q-2p)$$

which by definition of the Hurwitz zeta function (32) gives the desired estimate for q > 2p + 2.  $\Box$ 

In order to prove visualization of our solution, we have to truncate it not only up to some fixed index  $N = \operatorname{Index}(\alpha)$ , but also up to some fixed  $M = |\alpha| = \alpha_1 + \alpha_2 + \cdots + \alpha_n$ . Let us define another truncated chaos expansion with  $P_{N,M}(t,\omega) = \sum_{\operatorname{Index}(\alpha) \leq N} \sum_{|\alpha| \leq M} P_{\alpha}(t) H_{\alpha}(\omega)$ , and provide a norm error estimate for it in the next theorem.

**Theorem 2.2.** Let  $N, M \in \mathbb{N}_0$  and  $\zeta(\cdot, \cdot)$  be the Hurwitz zeta function defined by (32). The norm error estimate of the truncated chaos expansion  $P_{N,M}(t,\omega)$  is given by

$$||P(t,\omega)-P_{N,M}(t,\omega)||^2_{C([0,T],[-L,L]^6)\otimes(FS)_{-s,-q}}\leq \frac{1}{2^{q-2p}-1}\frac{\zeta(q-2p-1,N+1)}{2^{(q-2p)(M+1)}},\quad s\geq r^5,\ q>2p+2,$$

where r and p are chosen so that (25) is satisfied.

*Proof.* Once more we exploit the obtained inequality in the proof of Theorem 1.4, thus for some q > 2p + 1,

$$||P(t,\omega) - P_{N,M}(t,\omega)||^2_{C([0,T],[-L,L]^6)\otimes (FS)_{-s,-q}} \leq \sum_{\text{Index}(\alpha) > N} \sum_{|\alpha| > M} (2\mathbb{N})^{(2p-q)\alpha}.$$

Now, by applying similar ideas as in the proof of Theorem 2.1, we obtain that

$$\begin{split} \sum_{\text{Index}(\alpha)>N} \sum_{|\alpha|>M} (2\mathbb{N})^{(2p-q)\alpha} &= \sum_{n=N+1}^{\infty} \sum_{m=M+1}^{\infty} \sum_{\substack{\alpha_1,\alpha_2,\dots,\alpha_{n-1}\geq 0 \\ \alpha_1+\alpha_2+\dots+\alpha_n=m}}^{\infty} \prod_{j=1}^{n} (2j)^{(2p-q)\alpha_j} \\ &= \sum_{n=N+1}^{\infty} \sum_{m=M+1}^{\infty} \frac{1}{(2n)^{q-2p}} \sum_{k_1=1}^{n} \sum_{k_2=1}^{k_1} \cdots \sum_{k_m=1}^{k_{m-1}} (2k_1)^{2p-q} (2k_2)^{2p-q} \dots (2k_m)^{2p-q} \\ &\leq \sum_{n=N+1}^{\infty} \sum_{m=M+1}^{\infty} \frac{1}{(2n)^{q-2p}} n 2^{-(2p-q)m} \\ &= \sum_{n=N+1}^{\infty} \frac{1}{n^{q-2p-1}} \sum_{m=M+1}^{\infty} \frac{1}{2^{(q-2p)(m+1)}}, \end{split}$$

which gives the desired estimate for q > 2p + 2.  $\square$ 

By applying truncated chaos expansions i.e. finite partial sums, we approximate and simulate sample paths of the solution. To achive that, notice that  $H_{\epsilon^{(k)}}(\omega) = \langle \omega, \xi_k \rangle$  has a standardized Gaussian distribution for each  $k \in \mathbb{N}$ , see [21]. Hence, we simulate the polynomial basis by generating a sequence of normally distributed

pseudo-random numbers  $e_k$ ,  $k=1,2,\ldots,N$ , and consider  $\overline{P}_N(t)=\sum_{n=0}^N\sum_{\mathrm{Index}(\alpha)=n}^\alpha P_\alpha(t)\prod_{i=1}^n h_{\alpha_i}(e_i)$ , as a realization of the sample paths of the truncated solution

$$P_{N}(t,\omega) = \sum_{n=0}^{N} \sum_{\substack{\alpha \\ \text{Index}(\alpha)=n}} P_{\alpha}(t) H_{\alpha}(\omega) = \sum_{n=0}^{N} \sum_{\substack{\alpha \\ \text{Index}(\alpha)=n}} P_{\alpha}(t) \prod_{i=1}^{n} h_{\alpha_{i}}(\langle \omega, \xi_{i} \rangle),$$

where  $\omega \in S'(\mathbb{R})$ ,  $\alpha \in I$ . Indeed, by Theorem 2.1, it is reasonable to consider  $P_N(t,\omega)$  as an approximation of the solution  $P(t,\omega)$ , since  $\|P(t,\omega) - P_N(t,\omega)\|_{C([0,T],[-L,L]^6)\otimes (FS)_{-s,-q}} \to 0$  as  $N\to\infty$ , for any  $s\geq r^5$  and q>2p+2, where p and r satisfy (25). However, the truncated sum  $P_N(t,\omega)$  is still infinite since there is an infinite number of multiindexes that satisfy condition  $\mathrm{Index}(\alpha)\leq N$ , so we are forced to define another truncation, some  $M=|\alpha|=\alpha_1+\alpha_2+\cdots+\alpha_n,\ n\leq N$ , and consider  $P_{N,M}(t,\omega)$  as a finite sum that approximates the theoretical solution. Theorem 2.2 implies that  $P_{N,M}(t,\omega)$  converges to our solution as both parameters N and M tend to infinity.

#### 2.2. Numerical simulations of the aerosol diffusion

Now we turn to the simulation part with particularly chosen data that fit physical conditions such as room temperature, aerosol density etc. For the initial conditions of our model we take U(0) = (0,0,0) and X(0) = (0,0,0). In order to derive the constants A,B,C and k, let us impose that the initial conditions of the Navier-Stokes equation (1) are given by u(X(0),0) = (2,1/5,1/10). After we apply the Trkal solution (2), it implies that A = 1/5, B = 1/10, and C = 2 and to ensure that matrix S(t) has determinant different from zero, we choose k = 1/3. Hence, for such a choice of constants A,B,C, and k, there exists an unique solution  $P(t,\omega) = \sum_{\alpha \in I} P_{\alpha}(t)H_{\alpha}(\omega)$ , which belongs to the space  $C([0,T],[-L,L]^6) \otimes (FS)_{-s,-q}$ , for some s and q. The figures in the sequel are obtained for the approximation with N = 750 and M = 2,

$$\begin{split} \overline{P}_{750,2}(t) &= P_{\mathbf{0}}(t) + \sum_{|\alpha|=1}^{2} P_{\alpha}(t) \prod_{i=1}^{750} h_{\alpha_{i}}(e_{i}) \\ &= P_{\mathbf{0}}(t) + \sum_{i=1}^{750} P_{\epsilon^{(i)}}(t)e_{i} + \sum_{\substack{k,j \\ k \neq j}}^{750} P_{\epsilon^{(k)} + \epsilon^{(j)}}(t)e_{k}e_{j} + \sum_{i=1}^{750} P_{2\epsilon^{(i)}}(t)(e_{i}^{2} - 1), \end{split}$$

for different values of the Hurst parameter, Caputo-Fabrizio fractional order, and polynomial bases. Notice that  $P_0(t)$  is of particular interest since  $E[P(t,\omega)] = P_0(t)$ . To obtain the solution of the system (10)-(11) i.e. to calculate  $P_{\epsilon^{(j)}}(t)$ , it is necessary to approximate integrals

$$\frac{1}{\Gamma(H+\frac{1}{2})}\int_0^t \frac{d}{ds}\int_{-\infty}^s \xi_j(\tau)(s-\tau)^{H-\frac{1}{2}}d\tau ds, \quad \frac{1}{\Gamma(H+\frac{1}{2})}\frac{d}{dt}\int_{-\infty}^t \xi_j(\tau)(t-\tau)^{H-\frac{1}{2}}d\tau.$$

In order to achive that, we make use of chaos expansions of  $W^H(t,\omega)$  and  $B^H(t,\omega)$  (see (C.1),(C.2),(C.3)), i.e. of its three dimensional counterparts given by (4), which coefficiants are those integrals. Thus, with the aim of obtaining integral approximations, truncated sums  $\overline{W}_{250}^H(t)$  and  $\overline{B}_{250}^H(t)$  are applied, since the solution is simulated by 750 additions,

$$\overline{W}_{250}^{H}(t) = \sum_{j=1}^{250} \sum_{k=1}^{250} b_{j,k} \xi_j(t) (e_{1+3(k-1)}, e_{2+3(k-1)}, e_{3k})^T,$$
(32)

$$\overline{B}_{250}^{H}(t) = \sum_{j=1}^{250} \sum_{k=1}^{250} c_{j,k} \xi_j(t) (e_{1+3(k-1)}, e_{2+3(k-1)}, e_{3k})^T.$$
(33)

A norm error estimate for  $P_{750,2}(t,\omega)$  can be derived by Theorem 2.2, all that is needed are precise lower bounds for the parameters s and q. By Theorem 1.4,  $p \ge \widetilde{p} > g > 1$ , and  $r > r_0$ , where  $r_0$  is equal to (26). The chosen initial conditions for our model imply by (24) that  $\widetilde{r} > 2$ ,  $\widetilde{p} > 1$  and K = 0. On the other hand, the obtained values of A = 1/5, B = 1/10, C = 2 and k = 1/3 give that D = 1/4, and  $\max\{A, B, C\} = 2$ . Physical parameters are taken from Appendix G,  $\kappa_1 = \kappa_2 = 5/4 \cdot 10^{-5}$ , and  $\tau = 0.0016$ , while time and fractional order are elected to be T = 20 and  $\alpha = 0.9$ . In order to obtain values for  $\|N\|$ ,  $\|S(0)\|$ , and  $\|S^{-1}\|$ , recall that throughout the paper, we have been using norm  $\|\cdot\|_1$  for vectors and vector valued functions, so the induced matrix norm is the same one. Therefore, by (15) and (14), we get that  $\|N\| = 2250$ ,  $\|S(0)\| = 253/3$ , and  $\|S^{-1}\| = 3.1605$ . Moreover, by Lemma A.3,  $M = \pi^{-\frac{1}{4}}$ , and  $G^H(T) = 20$ , for Hurst parameter  $H = \frac{1}{2}$ . To sum up, it is obtained that  $r > r_0 = 4 + 41540e^{142222.5}$ , which implies that for  $s \ge r^5 > (4 + 20770e^{142222.5})^5$  and q > 2p + 2, norm estimates from Theorem 2.1 and Theorem 2.2 can be applied, hence for the particular value of q - 2p = 3, we obtain the error estimate

 $||P(t,\omega) - P_{750,2}(t,\omega)||_{C([0,T],[-L,L]^6)\otimes (FS)_{-s,-q}} \le 0.0006097.$ 

The results of the simulation of the sample paths  $\overline{P}_{750,2}(t)$  are presented on the following figures. Figure 1 illustrates how different fractional derivative orders have an effect to sample paths of a droplet. Note, as the Caputo-Fabrizio fractional order  $\mathfrak a$  increases, the sample path has a longer delay. The figures depict what we expect from experience, droplets tend to progress in an almost linear fashion up front (x direction) and to the side (y direction), while gravity pulls down the droplets resulting in a curved progress to downwards (z direction). Diametar of droplets are taken to be equal to  $10^{-5}m$ . From Figures 2, 3, and 4, we can see that as the Hurst parameter H increases, droplets have a larger dispersion. The Hurst parameter, too, has weakest effect in the frontal x direction and largest effect in the downwards z direction where the Naviere-Stokes airflow wears down and the collision events with air molecules and other particles have more influence than in the beginning. We point out that these values of  $\mathfrak a$  and H are chosen for illustrative purposes only, they are not fitted to real data.

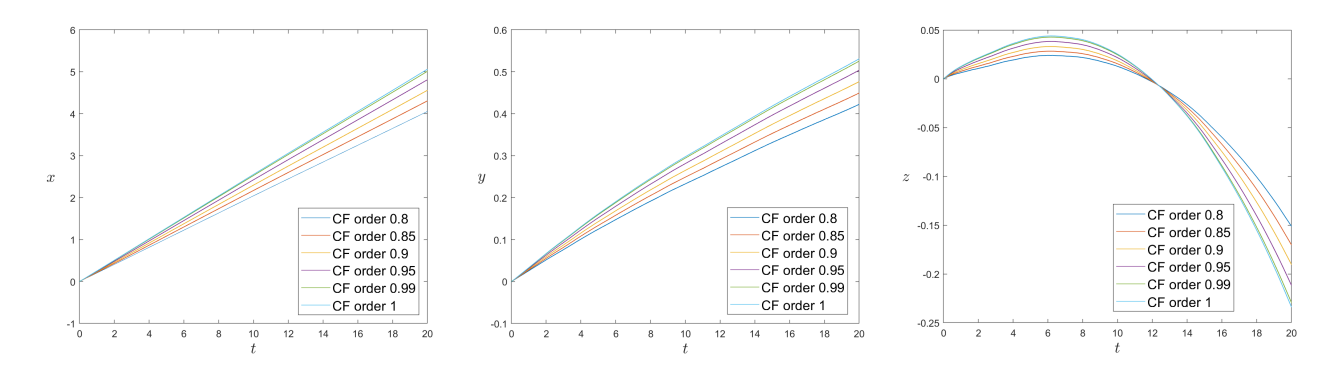


Figure 1: Simulation of the sample path of an individual droplet exhaled from mouth during first 20s along all three axes, for different fractional order, fixed Hurst parameter  $H = \frac{1}{2}$  and fixed polynomial basis.

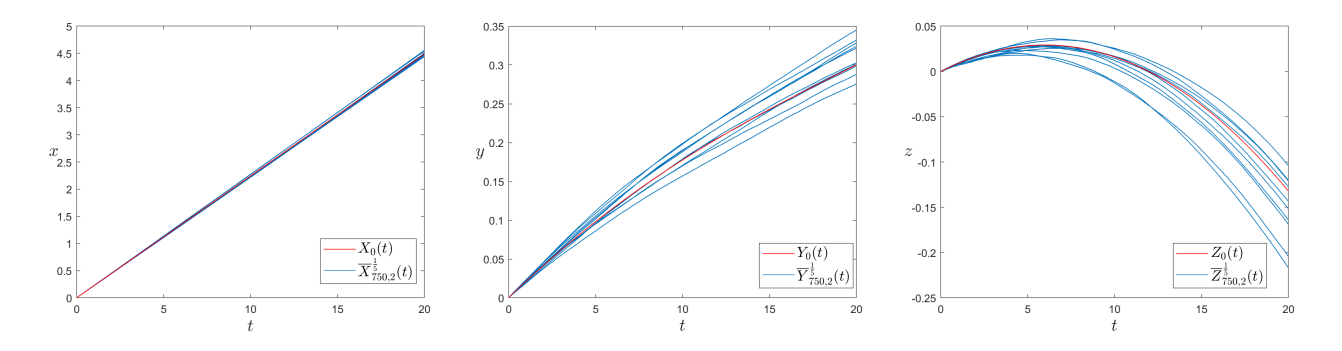


Figure 2: Simulation of the sample paths of several droplets during first 20s along all three axes, obtained for Caputo-Fabrizio fractional order  $\mathfrak{a}=0.9$ , and fixed Hurst parameter  $H=\frac{1}{5}$ . Blue lines correspond to several realizations of the models sample paths, while the red one corresponds to the expected trajectory.

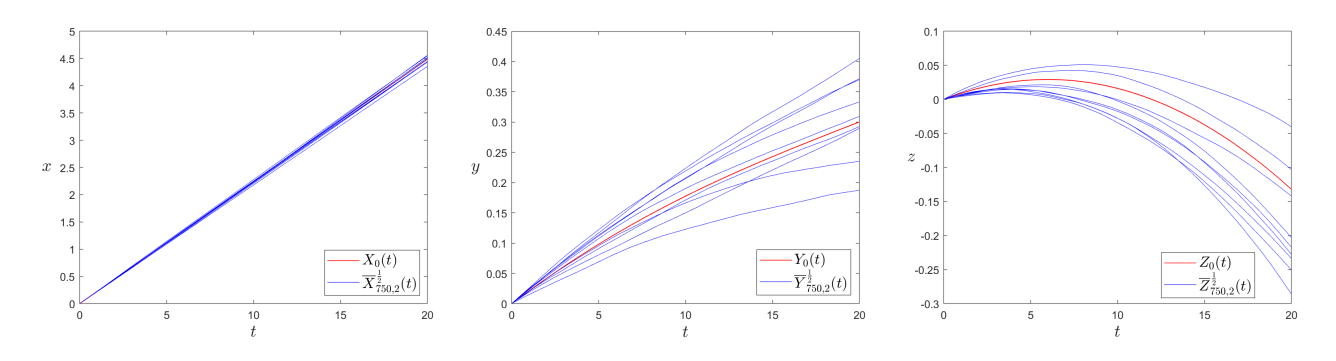


Figure 3: Simulation of sample paths of several droplets during first 20s along all three axes, obtained for Caputo-Fabrizio fractional order  $\mathfrak{a}=0.9$ , and fixed Hurst parameter  $H=\frac{1}{2}$ . Blue lines correspond to several realizations of the models sample paths, while the red one corresponds to the expected trajectory.

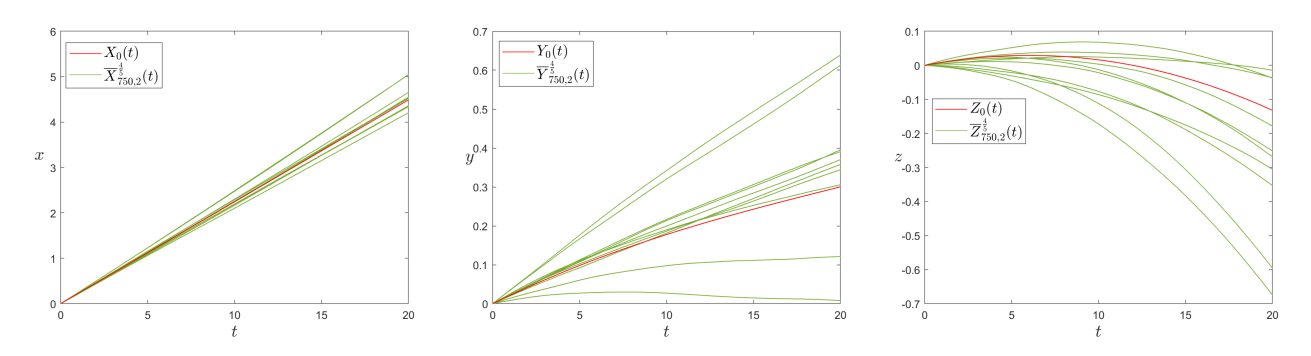


Figure 4: Simulation of sample paths of several droplets during first 20s along all three axes, obtained for Caputo-Fabrizio fractional order a = 0.9, and fixed Hurst parameter  $H = \frac{4}{5}$ . Green lines correspond to several realizations of the models sample paths, while the red one corresponds to the expected trajectory.

Finally, in Figure 5 we simulate a snapshot of 50 aerosols exhaled during the cough (up to 5000 are exhaled during regular cough), and give their positions in four fixed time moments. Let us stress that the initial radii of droplets for all 50 aerosols are taken randomly from 1 to  $50\mu m$ . Obviously, as time goes on, the

dispersion of aerosols increases. The red dot in those four figures corresponds to the expected position, i.e. to  $P_0$ . All figures are produced for  $\kappa_1 = \kappa_2 = D_\nu/2$ , where  $D_\nu$  is given in the Appendix G. With an increase of these two parameters the diffusion would increase and the droplet swarm would get more scattered in time.

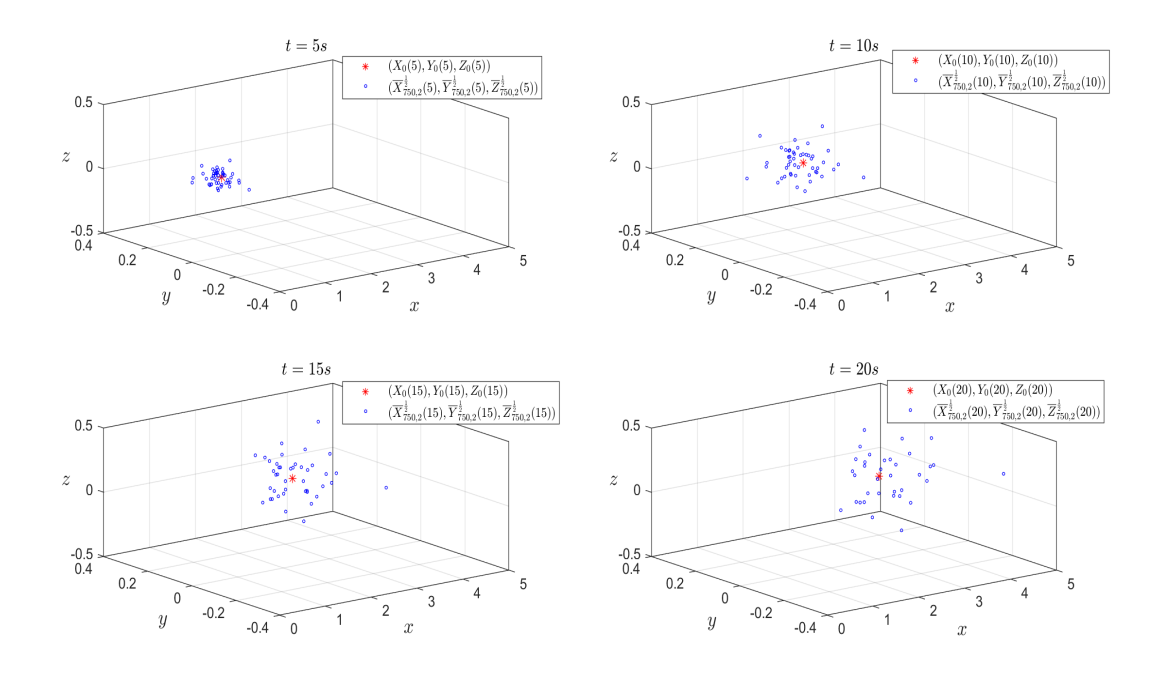


Figure 5: Snapshot of the expiratory event 5*s*, 10*s*, 15*s*, and 20*s* after start of coughing obtained from our numerical solution, for Hurst parameter  $H = \frac{1}{2}$  and Caputo-Fabrizio fractional order  $\alpha = 0.9$ .

#### 3. Model validation

Since the major goal of our work is to model turbulent transport of droplets, we recall and point out the two primary physical actors that are involved in that process. On the one hand, it is the airfow and turbulence, while on the other hand it is the humidity field and droplet evaporation. Firstly, let us say a few words about the physical properties of the exhaled air through coughing. Namely, each cough has a limited duration, and we need to distinguish between two different stages for the evolution of the exhaled airflow. In the first stage, which is known as the jet phase, the mouth is open and the source is still pushing the air out into space. The second stage, known as the puff phase, starts when the airflow or the cloud has lost its source, i.e. when the mouth is closed, and the droplets begin freely to spread through airspace. By [6], [19] a typical cough lasts around 0.2-0.5s, and the average mouth opening area is  $(4\pm0.95)cm^2$ , while the peak velocity of air is about 13m/s, which results in an extremely high Reynold number  $10^4$ . In order to validate the presented model, we take some results that were obtained in research [17], and the rich database of images collected therein and given in the repository of that paper. The research material includes video recordings of actual people breathing, breathing heavily, or coughing, both with and without face covering masks. Among the 280 tests, in which they aimed to examine how different surgical masks prevent or reduce the spreading of aerosol dispersion and lessen virus transmission risk, two are of particular interest to us. Namely, test No. 188 presents a man in standing position and test No. 253 presents a woman in a sitting position, both of them while coughing and without wearing a mask. The images and videos in [17] were obtained by the Background Oriented Schlieren (BOS) technique, which is an optical method used to visualize and measure refractive index variations in a transparent medium (in this case in the air) that are caused by density gradients in fluid flows (in this case the exhaled air from the mouth). To simulate the airflow generated by those two persons, we impose the inlet air velocities for the proposed Trkal solution by considering the results obtained in [17]. In both tests, the peak velocity in the x direction is around 8m/s, while along the z axis it is in both cases negative and equal to -0.2m/s and -2m/s, respectively for test No. 188 and test No. 253. Since we do not have any information about direct measurements along the y direction, we suppose that particles spread along the y axis with an initial velocity uniformly distributed between -1/5 and 1/5m/s. For these assumptions, the obtained constants for tests No. 188 and No. 253 are B=-1/2, C=-5.2, and B=-2, C=7.5, respectively, while  $A\sim\mathcal{U}(-1/5,1/5)$  for both tests. In order to provide the greatest degree of matching between the test results and our model, the constant *k* is taken to be k = 1/3 for test No. 188, and k = -1/3 for test No. 253. All droplets are initially at rest, which implies that the initial conditions for velocity in each direction are equal to zero. The results (images) from the tests are given in boxes with a range given in meters and equal to  $[-0.575, 0.65] \times [-0.175, 0.575]$ . The air is injected out through a mouth opening of area  $\approx 5cm^2$ , which is simulated in our model by a sphere of diameter 2.6cm centered in (0.4, 0.225) and (0.475, 0.375) respectively for test No. 188 and test No. 253. As we stated at the beginning, droplet transmission depends also on the humidity field and droplet evaporation rate in addition to the injected airflow through the mouth and turbulence. Since these factors are not ruled in our model, a lack of information is evident about how evaporation influences the size of injected droplets and further how it influences their transport process. By [15], it is known that the initial size of droplets is between  $1-1000\mu m$ , but due to evaporation in the jet phase (where the air is saturated) it drops to  $1-50\mu m$ . Thus, in our model we take that the size of droplets is randomly distributed to follow the histogram given in the figure below.

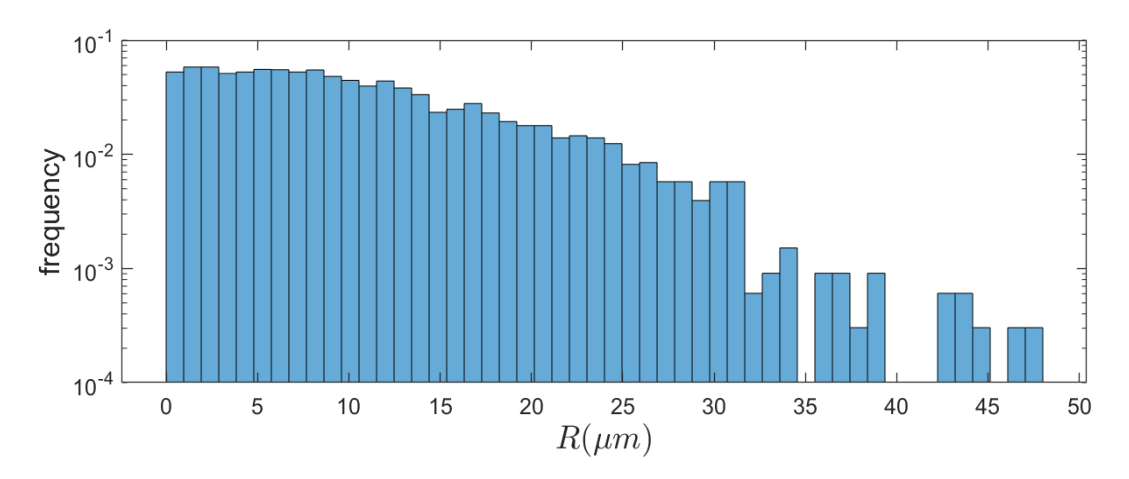


Figure 6: Distributon of initial radius size for droplets according to [40].

In addition to the mentioned initial conditions for the airflow and for the droplets, as well as for the system of equations of the model, we use the same truncation of the solution as in the previous section  $\overline{P}_{750,2}(t)$ . The results for test No. 188 are fitted for the Caputo-Fabrizio fractional order  $\alpha = 0.87$ , and the Hurst parameter H = 4/5, whereas the results for test No. 253 are fitted for  $\alpha = 0.9$  and H = 7/8. To validate our model and perform the final comparison, we present frames of the two prominent tests, as provided in the database available in [17], both captured in time at moment t = 1.2s after the cough started, juxtaposed to the simulations provided by our model as presented on Fig. 7 and Fig. 8.

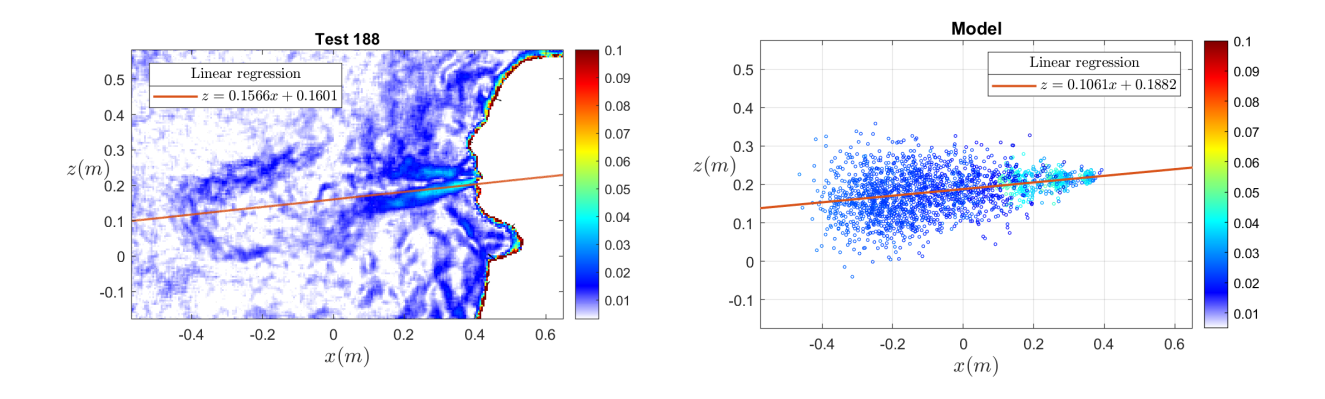


Figure 7: Left: Exhaled cloud 1.2 seconds after coughing in test No. 188 given in [17], with linear regression z = 0.1566x + 0.1601. Right: Cloud of 5000 droplets 1.2 seconds after coughing started, obtained from the model for A uniformly distributed between -1/5 and 1/5, B = -1/2, C = -5.2,  $\alpha = 0.87$  and H = 4/5, with obtained linear regression z = 0.1061x + 0.1882.

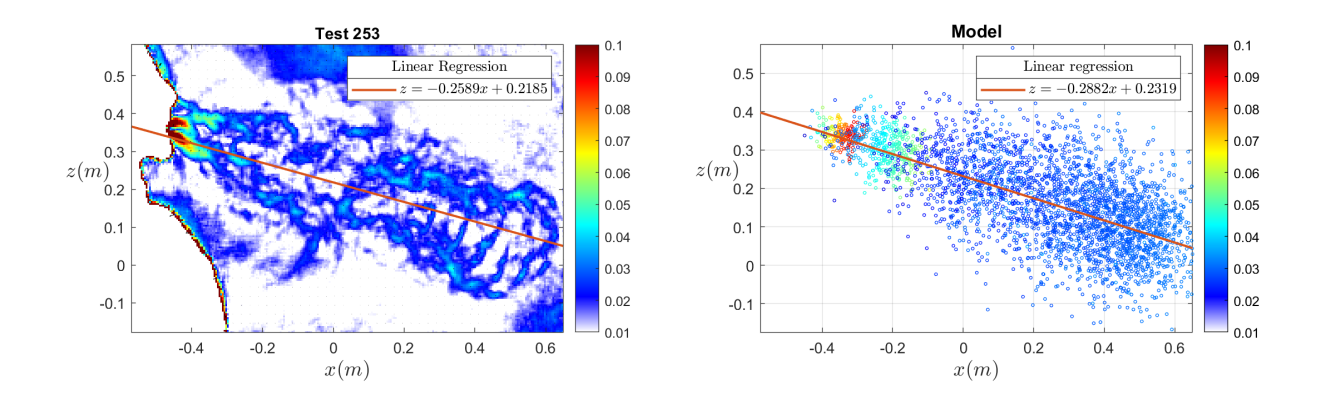


Figure 8: Left: Exhaled cloud 1.2 seconds after coughing in test No. 253 given in [17], with linear regression z = -0.2589x + 0.2185. Right: Cloud of 5000 droplets 1.2 seconds after coughing started, obtained from the model for for A uniformly distributed between -1/5 and 1/5,, B = -2, C = 7.5,  $\alpha = 0.9$  and H = 7/8, with obtained linear regression z = -0.2882x + 0.2319.

The left part of the figures stands for the realistic scenario according to the results provided in the database with a linear regression as estimation of the droplet propagation, while the right part of the figures corresponds to the simulated clouds of droplets by using our theoretical model and its truncated solution. By comparing those pairs of linear regressions we may observe that the errors are given as in Table 1. In the context of BOS, displacement refers to the apparent shift of background points when viewed through a medium with varying refractive index. This shift is caused by the deflection of light rays as they pass through regions with different refractive indices, which in turn are related to density variations in the

medium. The displacement observed in BOS is proportional to the integral of the density gradient along the optical path, indicating that regions with higher density gradients cause larger displacements of the background pattern. Although this displacement is not directly related to the velocity of the airflow and the aerosols therein, rather it measures the  $L^2$ -norm of the density gradient, it can be used as an approximate metric to indicate what happens with the particles' velocities.

The displacement of the exhaled droplets and room airflows in both images is measured by the density gradient given by  $(u_x(t)^2 + u_z(t)^2)^{\frac{1}{2}}$ , where  $u_x(t)$  and  $u_z(t)$  are displacements along the x and z axes at a moment t. It is then scaled to the interval [0,0.1] and color-coded via the heat legend, i.e. color-bar on the right of each figure. If we take a look at the realistic scenario images obtained from the tests we notice that the displacement of particles is the highest at the beginning of the clouds, around the mouth, which corresponds to the red color. Afterwards, it becomes lower as the speed of the exhaled airflow starts losing momentum, which corresponds to the color blue. The figures obtained in the simulations corresponding to our theoretical model also follow the same logic. Indeed, by using the same approach, droplets are colored with respect to their displacement scaled to the same interval, and derived by the norm of the gradient calculated as

$$\left( (X(t + \Delta t) - X(t))^2 + (Z(t + \Delta t) - Z(t))^2 \right)^{\frac{1}{2}}, \text{ for } \Delta t = 0.01.$$

In comparison to the realistic scenario of test images No. 188 and No. 253, our model captures very well the displacement and projected trajectories of the aerosol particles, as proven by the regression models and low error rates. It also captures the global behavior of the displacements of the aerosol swarm particles. A negligible imperfection of the model is that it does not perfectly capture the local behavior of the displacements, i.e. the gradient colors in the test images No. 188 and No. 253 are more mixed further away from the mouth, which is a consequence of the vorticity field that produces micro-local turbulences. Our model does not provide that kind of behavior of droplets, the gradient colors on the simulation images exhibit a more radial propagation. The reason for that lies in the assumption that in our model velocity and vorticity fields are aligned i.e.  $\partial \times u = u$ , which implied that the airflow exhaled from the mouth follows a Trkal flow. However, this assumption was necessary to obtain the nonlinear stochastic chaos expansion solutions in a closed form, tractable by the Wick product model. Since no model can ever be perfect, only an approximation of reality, the micro-local airflow turbulences were neglected as minor contributors of the global spreading of aerosol particles.

#### Conclusion and discussion

In recent years, the study of aerosol dispersion within closed spaces has gained significant attention due to its implications in various fields, including indoor air quality management, pollutant control, and public health. Accurate modeling of aerosol transport and dispersion in such environments is crucial for understanding the spread of contaminants and designing effective mitigation strategies. Traditional mathematical models based on ordinary or partial differential equations have been extensively used for this purpose. However, these models often fail to capture the complex behaviors observed in real-world

Linear regressions							
z = kx + n	Test No. 188	Model	Error	Test No. 253	Model	Error	
k	0.1566	0.1061	0.0505	-0.2589	-0.2882	0.0293	
п	0.1601	0.1882	0.0281	0.2185	0.2319	0.0134	

Table 1: Error estimates for the regression coefficients.

scenarios. To overcome the limitations of traditional models, there has been a growing interest in incorporating fractional calculus and stochastic processes into the field of aerosol dispersion modeling. Fractional derivatives provide a powerful tool for describing anomalous diffusion phenomena that are not adequately captured by classical derivative operators. On the other hand, stochastic differential equations offer a natural framework for accounting for the inherent randomness and uncertainty present in aerosol dispersion processes.

In this paper, we proposed a novel approach that combines fractional derivatives and stochastic differential equations to model aerosol dispersion in closed spaces. Specifically, we leveraged the Navier-Stokes equations as a foundation for our modeling framework, combined with the Wiener-Itô chaos expansion methods and the Caputo-Fabrizio derivative to propose a novel fractional stochastic model. The underlying SPDE system was solved via polynomial chaos expansions in the manner of white noise analysis, completely avoiding the classical Itô calculus. By expanding all terms in the SPDE into formal sums and taking orthogonal projections, it has transformed into an infinite system of PDEs. Due to the nice properties of the Wick product, this system was lower triangular and hence could be solved by recursion. In this manner we have obtained all coefficients in the chaos expansion of the solution sought. Controlling and estimating the growth rate of these coefficients was necessary to prove the convergence of the series. Due to the complexity of the model equation, i.e. the Wick-nonlinearities in the airflow equation u, it has been important to properly estimate also sums of finite products of the previous solutions in the recursion scheme. Solution to the model SPDE was hence obtained in form of an infinite series, with the fixed stochastic orthogonal basis  $H_{\alpha}$ . From a numerical point of view, this was also very convenient for numerical approximations and simulations. For this purpose we have simulated a fixed number of pseudo-random numbers following the normal distribution, used them as arguments for the Hermite polynomials, inserted them into the obtained chaos expansion solution and truncated the series at a finite (large) number N. The model incorporated fractional Brownian motion as a model for random perturbations in the position and velocity of aerosol particles. Fractional Brownian motion has also been modeled by a novel approach based on a recursion formula obtained for its Hermite expansion. Finally, the rate of change of particle positions was modeled not by the ordinary derivative but the Caputo-Fabrizio fractional derivative. The nonsingular kernel of the Caputo-Fabrizio derivative is one of its most attractive features and it has made the computational issues somewhat more feasible. In contrast to the classical Caputo derivative that would require dealing either with the Laplace transform and its complex inverse or numerical approximate schemes for interpolated solutions, the Caputo-Fabrizio derivative has simply turned our model equations into a linear combination (more precisely convex combination w.r.t. a) of the original model with zeroth derivatives and an enhanced model with first derivatives.

Although some authors criticize the Caputo-Fabrizio derivative derivative for not having a singular kernel and for not being a true fractional derivative, rather being a pass filter [48], or that it cannot describe nonlocality and memory effects [45], we have found it to be still useful for modeling purposes since it echoes similar subdiffusion and superdiffusion effects as the classical Caputo and Riemann-Liouville fractional derivatives, which paired with the already complicated tools of stochastic calculus turned out as an extraordinary tool for viable calculations. The Wick product has also received some critiques for not capturing the property of probabilistic independence and for supposedly having statistical flaws. However, the Wick product, by replacing ordinary products, helps regularize integrals in the equation, ensuring that the solutions remain well-defined and physically meaningful, even in the presence of singularities. The Wick product also involves integrating over all possible outcomes or sample paths of the underlying stochastic processes. This integration captures the combined influence of random variables across the entire sample space, rather than focusing solely on individual outcomes or pointwise interactions. Similarly as fractional derivatives with memory effects capture the influence of past states or trajectories on current behavior, emphasizing the temporal evolution of processes, the Wick product captures the joint influence of random variables on overall system dynamics, emphasizing the collective behavior of stochastic processes across all possible outcomes. One important consequence is the unbiasedness of the solution to the model SPDE: The expected value of the SPDE is equal to the solution of the SPDE with no noise (in our case the zeroth coefficient in the chaos expansion).

The final simulations of the model illustrate all these effects and aerosol swarm diffusion scenarios under

various fractional orders and various Hurst parameter values. In comparison with real-life scenarios and video-captured BOS images of aerosol dispersion flows after coughing and sneezing events, our model has turned out to be a promising one that captures the nature of trajectories of the droplet diffusion in a computationally efficient way. At this point we have to note that the BOS images provide valuable qualitative insights into the airflow and mixing dynamics following a cough; the density gradient data help identify regions of turbulent mixing and potential pathways for aerosol dispersion. However, for precise aerosol measurements and tracking the individual trajectories of aerosol particles, additional methods and equipment would be required, such as aerosol detectors and direct aerosol sampling or particle image velocimetry (PIV) techniques, to which we did not have access.

Through this research, we have made a further step to enhance our understanding of aerosol dispersion processes, improve the accuracy of existing predictive models, and contribute to the development of more effective strategies for managing indoor air quality and mitigating airborne hazards.

## Acknowledgements

The authors are truly grateful to Prof. Ignazio Maria Viola for providing access to the huge database counting more than 250 GB of images and video recordings of coughing events captured by the BOS technique, as well as for giving his permission to reproduce the images of test No. 188 and No. 253 in our paper.

The authors gratefully acknowledge the financial support of the Ministry of Science, Technological Development and Innovation of the Republic of Serbia (Grants No. 451-03-137/2025-03/200125, 451-03-136/2025-03/200125, and 451-03-137/2025-03/200156), Faculty of Technical Sciences, University of Novi Sad (Grant No. 01-50/295) and the support of the Provincial Secretariat for Higher Education and Scientific Research of Vojvodina (Grant No. 142-451-2327/2021-01/02).

## **Competing Interests**

The authors declare that they have no known competing financial interests or personal relationships that could have appeared to influence the work reported in this paper.

## A. Hermite polynomials and Hermite functions with other auxiliary functions

For a comprehensive overview of known formulae related to Hermite polynomials we refer to [18]. Here we list their definition and some results obtained in our upcoming paper [42] that are used in the proofs of the simulation of fractional white noise and fractional Brownian motion.

**Definition A.1.** Let  $\tilde{h}_n$  denote the (physicist's) Hermite polynomials defined by

$$\tilde{h}_n(x) = (-1)^n e^{x^2} \frac{d^n}{dx^n} (e^{-x^2}), \quad n = 0, 1, 2, \dots$$
 (A.1)

and let  $\xi_n$  denote the Hermite functions given by

$$\xi_n(x) = \frac{1}{\sqrt{2^{n-1}(n-1)!}\sqrt{\pi}} e^{-\frac{x^2}{2}} \tilde{h}_{n-1}(x), \quad n = 1, 2, 3, \dots$$
(A.2)

Moreover, for  $H \in (0,1)$ , we define functions  $A_n^H : \mathbb{R} \to \mathbb{R}$  by

$$A_n^H(t) = \int_{-\infty}^t e^{-\frac{x^2}{2}} \tilde{h}_n(x)(t-x)^{H-\frac{1}{2}} dx, \quad n = 0, 1, 2, \dots,$$
(A.3)

and coefficients  $B_{j,k}^H \in \mathbb{R}$  with

$$B_{j,k}^{H} = \int_{-\infty}^{\infty} e^{-\frac{t^{2}}{2}} \tilde{h}_{j-1}(t) A_{k-1}^{H}(t) dt, \quad j,k = 1,2,3,\dots$$
(A.4)

**Lemma A.2.** For every  $t \in \mathbb{R}$ , the sequence  $A_n^H(t)$ ,  $H \in (0,1)$  satisfies the recursion relation

$$A_{n+1}^{H}(t) = -2\frac{d}{dt}A_{n}^{H}(t) - 2nA_{n-1}^{H}(t), \quad n = 1, 2, 3, \dots$$
(A.5)

Moreover, we know that for for n = 0, 1, 2, ...

$$A_n^H(t) = \sum_{k=0}^n \binom{n}{k} (-2)^{n-k} 2^{\frac{n}{2} - \frac{k}{2} + \frac{H}{2} - \frac{3}{4}} \Gamma\left(\frac{n}{2} - \frac{k}{2} + \frac{H}{2} + \frac{1}{4}\right) \tilde{h}_k(t) {}_1F_1\left(\frac{1}{4} - \frac{H}{2} - \frac{n}{2} + \frac{k}{2}; \frac{1}{2}; -\frac{t^2}{2}\right)$$

$$+ \sum_{k=0}^n \binom{n}{k} (-2)^{n-k} 2^{\frac{n}{2} - \frac{k}{2} + \frac{H}{2} - \frac{1}{4}} \Gamma\left(\frac{n}{2} - \frac{k}{2} + \frac{H}{2} + \frac{3}{4}\right) t \tilde{h}_k(t) {}_1F_1\left(\frac{3}{4} - \frac{H}{2} - \frac{n}{2} + \frac{k}{2}; \frac{3}{2}; -\frac{t^2}{2}\right). \tag{A.6}$$

**Lemma A.3.** There exists M > 0 such that for every t > 0, the function  $A_n^H(t)$ ,  $H \in (0,1)$ , satisfies

$$\frac{|A_n^H(t) - A_n^H(0)|}{\sqrt{2^n n! \sqrt{\pi}}} \le 4MG^H(t), \quad G^H(t) = \begin{cases} t^{H - \frac{1}{2}}, & t \in (0, 1), \\ t^{H + \frac{1}{2}}, & t \ge 1. \end{cases}$$
(A.7)

Theorem A.4. Let

$$a_{j,k}^{H} = \frac{B_{j,k}^{H}}{\sqrt{2^{j-1}(j-1)!\sqrt{\pi}}\sqrt{2^{k-1}(k-1)!\sqrt{\pi}}}, \quad j,k = 1,2,3,\dots,$$
(A.8)

with initial values given by

$$a_{j,1}^{H} = \frac{\Gamma\left(\frac{j}{2} + \frac{H}{2} - \frac{1}{2}\right)}{\Gamma\left(\lfloor\frac{j-1}{2}\rfloor + \frac{3}{2}\right)} \frac{(2\lfloor\frac{j-1}{2}\rfloor + 1)!!}{\sqrt{(j-1)!}} 2^{\lceil\frac{j-1}{2}\rceil - \frac{j}{2} + H - 1} \sqrt{\pi}, \quad j = 1, 2, 3, \dots,$$
(A.9)

$$a_{1,2}^{H} = -2^{H}\Gamma\left(\frac{H}{2} + \frac{3}{4}\right), \quad a_{j,2}^{H} = \frac{\Gamma\left(\frac{j}{2} + \frac{H}{2} - \frac{3}{4}\right)}{\Gamma\left(\lfloor\frac{j-1}{2}\rfloor + \frac{1}{2}\right)} \frac{(2\lfloor\frac{j-1}{2}\rfloor - 1)!!}{\sqrt{(j-1)!}} 2^{\lceil\frac{j-1}{2}\rceil - \frac{j}{2} + H - \frac{1}{2}} \sqrt{\pi}, \quad j = 2, 3, 4, \dots$$
(A.10)

*Then for j, k* = 2, 3, 4, ..., the numbers satisfy the recurrence relation

$$\sqrt{j}a_{j+1,k}^H + \sqrt{k}a_{j,k+1}^H - \frac{k}{\sqrt{k-1}}a_{j,k-1}^H - \frac{j}{\sqrt{j-1}}a_{j-1,k}^H = 0.$$

Moreover, for all  $j,k \in \mathbb{N}$  it follows that  $a_{j,k}^H = (-1)^{j+k} a_{k,j'}^H$  and

$$a_{jk}^{H} = \sum_{i=0}^{\lfloor \frac{k-1}{2} \rfloor} \frac{\sqrt{\pi} \sqrt{(k-1)!}}{(k-2i-1)!} 2^{\lceil \frac{j-1}{2} \rceil - \frac{j}{2} + \frac{3k}{2} - 3i + H - \frac{5}{2}} \times \sum_{l=0}^{(j-1) \wedge (2i+1)} \frac{\sqrt{(j-1)!}}{l!(j-l-1)!} \frac{(2\lfloor \frac{j-1}{2} \rfloor + 2i - 2l + 1)!!(3i - l - \frac{k}{2} + \frac{3}{2})}{(2i-l+1)!(-1)^{2i-k+1}} \frac{\Gamma\left(\frac{j}{2} + \frac{k}{2} - l + \frac{H}{2} - \frac{3}{4}\right)}{\Gamma\left(\lfloor \frac{j-1}{2} \rfloor + i - l + \frac{3}{2}\right)},$$
(A.11)

We note that the family  $\xi_n$ ,  $n \in \mathbb{N}$ , constitutes an orthonormal basis of  $L^2(\mathbb{R})$ , thus each function  $f \in L^2(\mathbb{R})$  has a unique representation  $f(t) = \sum_{j=1}^{\infty} f_j \xi_j(t)$ , where  $f_j = \int_{-\infty}^{\infty} f(x) \xi_j(x) dx$ ,  $j \in \mathbb{N}$ , and  $\sum_{j=1}^{\infty} |f_j|^2 < \infty$ . The Schwartz space of tempered distributions  $S'(\mathbb{R})$  consists of formal expansions of the form  $F = \sum_{j=1}^{\infty} c_j \xi_j$ ,  $c_j \in \mathbb{R}$ ,  $j \in \mathbb{N}$ , such that  $||F||_{S_{-p}(\mathbb{R})}^2 = \sum_{j=1}^{\infty} |c_j|^2 (2j)^{-p} < \infty$ , for some p > 0.

#### B. White noise space and Wiener-Itô chaos expansion

For the purpose of white noise analysis we use the (probabilist's) renormalization of the Hermite polynomials and define  $h_n(x) = 2^{-\frac{n}{2}}\tilde{h}_n(\frac{x}{\sqrt{2}})$ ,  $n = 0, 1, 2, \ldots$  The Gaussian white noise space [20] is defined on the probability space  $\Omega = S'(\mathbb{R})$  endowed with the Borel  $\sigma$ -algebra  $\mathcal{F}$  generated by the weak topology and the Gaussian measure  $\mu$  given by the Bochner-Minlos theorem. Let  $I = (\mathbb{N}_0^{\mathbb{N}})_c$  be the set of multiindeces and  $\varepsilon^{(k)} = (0, \cdots, 0, 1, 0, \cdots)$ ,  $k \in \mathbb{N}$ , the unit multiindeces. Let  $(L)^2 = L^2(S'(\mathbb{R}), \mathcal{F}, \mu)$  be the Hilbert space of random variables with finite second moments. Then,

$$H_{\alpha}(\omega) = \prod_{k=1}^{\infty} h_{\alpha_k}(\langle \omega, \xi_k \rangle), \quad \omega \in S'(\mathbb{R}), \ \alpha = (\alpha_1, \alpha_2 \dots) \in I,$$

constitutes the Fourier-Hermite orthogonal basis of  $(L)^2$ . The prominent Wiener-Itô chaos expansion theorem states that each element  $F \in (L)^2$  has a unique representation of the form  $F(\omega) = \sum_{\alpha \in I} c_\alpha H_\alpha(\omega)$ ,  $\omega \in S'(\mathbb{R})$ ,  $c_\alpha \in \mathbb{R}$ ,  $\alpha \in I$ , such that  $||F||_{(L)^2}^2 = \sum_{\alpha \in I} c_\alpha^2 \alpha! < \infty$ .

**Definition B.1.** The space of the Kondratiev generalized random variables  $(S)_{-1}$  consists of formal expansions of the form  $F = \sum_{\alpha \in I} b_{\alpha} H_{\alpha}$ ,  $b_{\alpha} \in \mathbb{R}$ ,  $\alpha \in I$ , such that

$$||F||_{(S)_{-1,-q}}^2 = \sum_{\alpha \in I} b_\alpha^2 (2\mathbb{N})^{-q\alpha} < \infty, \quad \text{for some } q > 0,$$

with respect to the weight factor  $(2\mathbb{N})^{\alpha} = \prod_{i=1}^{\infty} (2i)^{\alpha_i}$ .

**Definition B.2.** Generalized stochastic processes in sense of [24] are elements of the space

$$S'(\mathbb{R}) \otimes (S)_{-1} = \bigcup_{p,q \in \mathbb{N}} S_{-p}(\mathbb{R}) \otimes (S)_{-1,-q},$$

with expansion of the form  $F = \sum_{\alpha \in I} \sum_{j \in \mathbb{N}} f_{\alpha,j} \xi_j H_\alpha$ ,  $f_{\alpha,j} \in \mathbb{R}$ ,  $\alpha \in I$ ,  $j \in \mathbb{N}$ , such that

$$||F||_{X\otimes S_{-p}(\mathbb{R})\otimes (S)_{-1,-q}}^2 = \sum_{\alpha\in I} \sum_{j\in \mathbb{N}} |f_{\alpha,j}|^2 (2j)^{-p} (2\mathbb{N})^{-q\alpha} < \infty, \quad \text{for some } p,q>0.$$

## C. Fractional Brownian motion and fractional white noise

Important examples of generalized stochastic processes are fractional white noise and fractional Brownian motion with Hurst parameter  $H \in (0,1)$  that play a crucial role in modeling phenomena more complex than regular white noise and fractional Brownian motion.

**Theorem C.1.** Fractional white noise and fractional Brownian motion are respectively given by the chaos expansions

$$W^{H}(t) = \sum_{k=1}^{\infty} \sum_{j=1}^{\infty} b_{j,k} \xi_{j}(t) H_{\epsilon^{(k)}}(\omega), \quad B^{H}(t) = \sum_{k=1}^{\infty} \sum_{j=1}^{\infty} c_{j,k} \xi_{j}(t) H_{\epsilon^{(k)}}(\omega), \tag{C.1}$$

where the coefficients  $b_{j,k}$  and  $c_{j,k}$  can be expressed in terms of  $a_{i,k}^H$  (see Appendix (A)) as

$$b_{j,1} = \frac{1}{\Gamma(H + \frac{1}{2})} \left( -\frac{1}{\sqrt{2}} \right) a_{j,2}^{H},$$

$$b_{j,k} = \frac{1}{\Gamma(H + \frac{1}{2})} \left( -\sqrt{\frac{k}{2}} a_{j,k+1}^{H} + \sqrt{\frac{k-1}{2}} a_{j,k-1}^{H} \right), \quad k = 2, 3, 4, \dots,$$
(C.2)

and

$$c_{j,k} = \frac{1}{\Gamma(H + \frac{1}{2})} a_{j,k}^{H} - \frac{1}{\Gamma(H + \frac{1}{2})} \begin{cases} 0, & j = 2, 4, 6 \dots, \\ \frac{A_{k-1}^{H}(0)2^{\frac{j}{2}}\Gamma(\frac{j}{2})}{\sqrt{2^{k-1}(k-1)!}\sqrt{\pi}}, & j = 1, 3, 5, \dots \end{cases}$$
(C.3)

For a proof of these formulae we refer the readers to [42]. As generalized stochastic processes with expansions in  $b_{j,k}$  and  $c_{j,k}$ ,  $W^H(t,\omega)$  and  $B^H(t,\omega)$  must be regarded as elements of the space  $S'(\mathbb{R}) \otimes (S)_{-1}$ . This means that

$$||W^{H}||_{S_{-f}(\mathbb{R})\otimes(S)_{-1,-g}}^{2} = \sum_{k=1}^{\infty} \sum_{j=1}^{\infty} |b_{j,k}|^{2} (2j)^{-f} (2k)^{-g} < \infty,$$
(C.4)

$$||B^{H}||_{S_{-f}(\mathbb{R})\otimes(S)_{-1,-g}}^{2} = \sum_{k=1}^{\infty} \sum_{j=1}^{\infty} |c_{jk}|^{2} (2j)^{-f} (2k)^{-g} < \infty,$$
(C.5)

for some f,g > 1. Also, in sense of weak derivatives in  $S'(\mathbb{R})$  it holds that  $\frac{d}{dt}B^H(t) = W^H(t)$ . Finally, we note that for  $H = \frac{1}{2}$  one retrieves the classical white noise and classical Brownian motion case.

#### D. The Wick product

The Wick product is used in white noise analysis as a renormalization of the ordinary product, since generalized stochastic processes cannot be multiplied in the usual way (mirroring the famous Schwartz impossibility result). Hence, one has to take out the infinite (divergent) part of the ordinary product of two generalized random variables and restrict (or in terms of quantum physics to "renormalize") to the well-defined part of the product [20], [21], etc.

**Definition D.1.** The Wick product of two random variables  $X, Y \in (S)_{-1}$  in the chaos expansion form  $X = \sum_{\alpha} x_{\alpha} H_{\alpha}$ ,  $Y = \sum_{\beta} y_{\beta} H_{\beta}$ , is defined by

$$X \diamond Y = \sum_{\gamma} \left( \sum_{\alpha + \beta = \gamma} x_{\alpha} y_{\beta} \right) H_{\gamma}.$$

Furthermore, one can define also Wick-powers by letting  $X^{\Diamond n} = X \Diamond X^{\Diamond (n-1)}$ ,  $n \in \mathbb{N}$ .

The Wick product is inherently incorporated into the Itô integrals and Itô calculus, as one can see e.g. from  $\int_0^t B_s(\omega)dB_s(\omega) = \frac{1}{2}(B_t^2(\omega) - t^2) = \frac{1}{2}B_t^{\diamond 2}(\omega)$ . More generally,  $\int_0^t X_s(\omega)dB_s(\omega) = \int_0^t X_s(\omega) \diamond W_s(\omega)$  and the latter can be evaluated by usual Riemann integration rules. Due to its convolutional nature, the Wick product is non-local, that is the value of  $X(\omega) \diamond Y(\omega)$  depends not only on one outcome  $\omega$  but it involves integrating over all possible outcomes of the involved random variables, or integrating over all sample paths in case of stochastic processes.

In order to consider not only Wick-powers of random variables but also Wick-versions of analytic functionals of random variables and to solve SPDEs with such terms one has to relate to an even larger space of generalized random variables than the Kondratiev space. In [26] the authors have dealt with this situation, hence we recall the definition of the space (*FS*)' and results related to it.

**Definition D.2.** The space (FS)' consists of formal expansions of the form  $F = \sum_{\alpha \in \mathcal{I}} f_{\alpha} H_{\alpha}$ ,  $f_{\alpha} \in \mathbb{R}$ , such that

$$||F||_{(FS)_{-r,-p}}^2 = \sum_{\alpha \in I} \alpha! |f_\alpha|^2 (r^{|\alpha|^3}!)^{-1} (2\mathbb{IN})^{-p\alpha} < \infty, \quad \textit{for some } r \geq 2, \; p \geq 0.$$

This now allows to capture higher levels of singularity in generalized random variables, namely  $(S)_{-1} \subseteq (FS)'$ .

The Wick-version of analytic functionals of stochastic processes is straightforward to be considered following [21]. If  $\Phi$  is analytic at  $x_0 := E(X)$ , where  $X \in (FS)'$ , one can establish the Taylor expansion, i.e. there exists an infinite sequence  $a_n = \frac{\Phi^{(n)}(x_0)}{n!}$ ,  $n \ge 0$  such that  $\Phi(x) = \sum_{n=0}^{\infty} a_n(x-x_0)^n$ ,  $x \in U$ , where U is a neighborhood of  $x_0$ . Then the Wick version  $\Phi^{\diamond}(X)$  of  $\Phi$  applied to X is defined by

$$\Phi^{\diamond}(X) = \sum_{n=0}^{\infty} a_n (X - x_0)^{\diamond n}.$$

Furthermore, if  $\Phi$  is an entire function, then  $\Phi(x) = \sum_{n=0}^{\infty} a_n x^n$ , which implies that  $\Phi^{\diamond}(X)$  is defined for all  $X \in (FS)'$ , and we have

$$\Phi^{\diamond}(X) = \sum_{n=0}^{\infty} a_n X^{\diamond n}, \quad X \in (FS)'.$$

**Lemma D.3 ([26]).** *If*  $X \in C([0,T];\mathbb{R}^n) \otimes (FS)'$ , then  $\Phi^{\diamond}(X)$  is a well defined element of  $C([0,T];\mathbb{R}^n) \otimes (FS)'$  and it can be represented in the form

$$\Phi^{\diamond}(X)(t,\omega) = \sum_{n=0}^{\infty} a_n X^{\diamond n}(t,\omega) = \Phi(X_0(t)) H_0(\omega) + \sum_{|\alpha| > 0} \left( \Phi'(X_0) X_{\alpha}(t) + r_{\alpha,\Phi}(t) \right) H_{\alpha}(\omega), \tag{D.1}$$

where  $t \in [0, T]$ ,  $\omega \in \Omega$ . For  $\alpha \in I$ ,  $|\alpha| = 1$   $r_{\alpha, \Phi}(t) = 0$ ,  $t \in [0, T]$  and for  $\alpha \in I$ ,  $|\alpha| > 1$  the functions  $r_{\alpha, \Phi}$  are of the form

$$r_{\alpha,\Phi}(t) = \sum_{k=2}^{|\alpha|} \frac{\Phi^{(k)}(X_0(t))}{k!} \sum_{0 < \gamma_1 < \alpha} \sum_{0 < \gamma_2 < \gamma_1} \cdots \sum_{0 < \gamma_{k-1} < \gamma_{k-2}} X_{\alpha - \gamma_1}(t) X_{\gamma_1 - \gamma_2}(t) \cdots X_{\gamma_{k-2} - \gamma_{k-1}}(t) X_{\gamma_{k-1}}(t), \quad t \in [0, T], \quad (D.2)$$

so as one can see,  $r_{\alpha,\Phi}$  depends only on the coefficients  $X_{\beta}$ , for  $\beta < \alpha$ .

#### E. Caputo-Fabrizio fractional calculus

We refer to [8] for a more extensive overview of known formulas related to Caputo-Fabrizio fractional calculus. Here we list the formulas and definitions used in this article.

**Definition E.1.** For a function  $f \in H^1([0,T])$  the Caputo-Fabrizio fractional derivative of order  $0 < \mathfrak{a} < 1$ , is given by

$${}^{CF}D^{\mathfrak{a}}f(t) = \frac{1}{1-\mathfrak{a}} \int_0^t f'(\tau)e^{-\frac{\mathfrak{a}}{1-\mathfrak{a}}(t-\tau)}d\tau, \tag{E.1}$$

while the corresponding fractional integral is

$$^{CF}I^{a}f(t) = (1 - \mathfrak{a})[f(t) - f(0)] + \mathfrak{a}\int_{0}^{t} f(\tau)d\tau.$$
 (E.2)

**Lemma E.2.** The relation between the Caputo-Fabrizio fractional derivative and the corresponding integral is given by

$${}^{CF}I^{\alpha}({}^{CF}D^{\alpha}f(t)) = f(t) - f(0), \tag{E.3}$$

$${}^{CF}D^{\mathfrak{a}}({}^{CF}I^{\mathfrak{a}}f(t)) = f(t) - f(0)e^{-\frac{\mathfrak{a}}{1-\mathfrak{a}}t}. \tag{E.4}$$

Since  $\lim_{t\to 0+} {^{CF}D^{\mathfrak{a}}} f(t) = 0$  for all functions, ODEs of the form  ${^{CF}D^{\mathfrak{a}}} y(t) = g(t)$  need to satisfy g(0) = 0 as a compatibility criterion for well-posedness. For  $g(0) \neq 0$  equations can be regularized by  ${^{CF}D^{\mathfrak{a}}} y(t) = g(t) - g(0)$  or even better by  ${^{CF}D^{\mathfrak{a}}} y(t) = g(t) - g(0)e^{-\frac{\mathfrak{a}}{1-\mathfrak{a}}t}$ . In contrast to the classical Caputo derivative where the first derivative f' is convoluted with a singular kernel  $t^{-\mathfrak{a}}$ , the Caputo-Fabrizio definition uses a regular kernel  $e^{-\frac{\mathfrak{a}}{1-\mathfrak{a}}t}$  for this purpose. Note that this function is also in the kernel of the integral operator, i.e.,

$${}^{CF}I^{\alpha}\left(e^{-\frac{\alpha}{1-\alpha}t}\right) = 0. \tag{E.5}$$

#### F. On matrix and vector valued functions

In order to stay clear about notation related to matrix and vector valued functions we enlist several rules and definitions. Let  $S(t), N(t) : \mathbb{R} \to \mathbb{R}^{n \times m}$ ,  $N(t) : \mathbb{R} \to \mathbb{R}^{m \times k}$  be given by  $S(t) = [S_{ij}(t)]_{n \times m}$ , and  $N(t) = [N_{ij}(t)]_{m \times k}$ . Differentiation of matrices acts componentwise as  $\frac{d}{dt}S(t) = [\frac{d}{dt}S_{ij}(t)]_{n \times m}$  and  $\frac{d}{dt}N(t) = [\frac{d}{dt}N_{ij}(t)]_{m \times k}$ , and the Leibniz rule holds:

$$\frac{d}{dt}\left(S(t)N(t)\right) = \frac{d}{dt}S(t)N(t) + S(t)\frac{d}{dt}N(t). \tag{F.1}$$

For two matrices  $F, H \in \mathbb{R}^{n \times n}$ ,  $F = [f_{ij}]_{n \times n}$ ,  $H = [h_{ij}]_{n \times n}$ , we say that F is dominated by H, and we write  $F \le H$ , if  $f_{ij} \le h_{ij}$  holds for any pair i, j = 1, ..., n, while the absolute value of a matrix F is considered as  $|F| = [|f_{ij}|]_{n \times n}$ .

The space  $C([0,T],[-L,L]^6)$  for T>0, L>0, consists of vector valued functions  $P(t):[0,T]\to[-L,L]^6$  given by  $P(t)=(P_1(t),\ldots,P_6(t))$ , such that

$$||P(t)||_{C([0,T],[-L,L]^6)} = \sup_{t \in [0,T]} ||P(t)||_{[-L,L]^6} = \sum_{i=1}^6 \sup_{t \in [0,T]} |P_i(t)|, \tag{F.2}$$

where we have choosen the norm 1 on  $[-L, L]^6$ . Notice, we could pick any other norm since all norms are equivalent on finite-dimensional spaces.

The following theorem provides a linear generalization of Grönwall's inequality, for more details see [9].

**Theorem F.1.** Let G(t) and H(t) be square, continuous, and nonnegative matrices for  $t_0 < t$ . If

$$U(t) \le a(t) + G(t) \int_{t_0}^t H(s)U(s)ds, \quad t_0 < t,$$

then

$$U(t) \le a(t) + G(t) \int_{t_0}^t V(t,s)H(s)a(s)ds, \quad t_0 < t,$$

where V(t,s) satisfies,

$$V(t,s) = I + \int_s^t H(r)G(r)V(r,s)dr, \quad t_0 < s < t.$$

Moreover, if H(t) := H and G(t) := G are constant matrices, it follows that  $V(t,s) = e^{(t-s)HG}$ .

## G. Physical and chemical properties of aerosols produced in expiratory events

The complete representation of physical and chemical parameters appearing in our model simulation in Section 2 is presented in the following table. For a more comprehensive view see [40].

Density of liquid water	$ ho_w$	$9.97 \times 10^2 kg/m^3$
Density of soluble aerosol part (NaCI)	$ ho_s$	$2.2\times10^3 kg/m^3$
Density of insoluble aerosol part (mucus)	$ ho_u$	$1.5 \times 10^3 kg/m^3$
Mass fraction of soluble material (NaCI) with respect to the total droplet	$\epsilon_m$	0.75
Mass fraction of dry nucleus with respect to the total droplet	С	1%
Diffusivity of water vapor	$D_{\nu}$	$2.5 \times 10^{-5} m^2/s$
Density of air	$\rho_a$	$1.18kg/m^3$
Kinematic viscosity of air	ν	$1.8 \times 10^{-5} m^2/s$
Initial diameter of a droplet	R	$10^{-6} - 10^{-3}m$

We point out that initial droplet radii, by [19] and [15], is approximately from 1 to  $1000\mu m$ . Due to evaporation, almost 95% of them are falling between 1 and  $50\mu m$ , so that is the droplet range used in all simulations.

By using the listed parameters, we derive  $\tau$ , Stokes relaxation time of the droplet for given R as its radius. The overall density of the dry nucleus can be expressed as

$$\rho_N = \frac{\rho_u}{1 - \epsilon_m (1 - \rho_u/\rho_s)} = 1.97 \times 10^3 kg/m^3,$$

while the density of the entire droplet turns out to be

$$\rho_D = \rho_w + (\rho_N - \rho_w) \left(\frac{r_N}{R}\right)^3,$$

where the radius of the dry solid part of the droplet is given by

$$r_N = R \left( \frac{C\rho_w}{C\rho_w + \rho_N(1 - C)} \right)^{1/3}.$$

Finaly, the Stokes relaxation time is equal to

$$\tau = \frac{2\rho_D R^2}{9\rho_a \nu}.$$

## References

- [1] A.M. Sayed Ahmed, M. Hamdy Ahmed, A. Taher Nofal, Adel Darwish, and A.M Othman Omar. Hilfer-Katugampola fractional epidemic model for malware propagation with optimal control. *Ain Shams Engineering Journal*, 15:102945, 2024.
- [2] M. Hamdy Ahmed, A. Reda Elbarkouky, A.M Othman Omar, and Maria Alessandra Ragusa. Models for COVID-19 daily confirmed cases in different countries. *Mathematics*, 9:659, 2021.
- [3] Kholoud Albalawi and Ibtehal Alazman. On study of modified Caputo–Fabrizio omicron type COVID-19 fractional model. Fractal and Fractional, 6:517, 09 2022.
- [4] T. Atanacković, S. Pilipović, and D. Zorica. Properties of the Caputo-Fabrizio fractional derivative and its distributional settings. Fractional Calculus and Applied Analysis, 21(1):29–44, 2018.
- [5] David Barbato, Luigi Berselli, and Carlo Grisanti. Analytical and numerical results for the rational large Eddy simulation model. Journal of Mathematical Fluid Mechanics, 9:44–74, 01 2007.

- [6] Lydia Bourouiba, Eline Dehandschoewercker, and John Bush. Violent expiratory events: On coughing and sneezing. *Journal of Fluid Mechanics*, 745, 03 2014.
- [7] Alexandre Caboussat. Mathematical modeling of atmospheric flow and computation of convex envelopes. *Mathematical Modelling of Natural Phenomena*, 6:44 66, 01 2011.
- [8] Michele Caputo and Mauro Fabrizio. A new definition of fractional derivative without singular kernel. *Prog Fract Differ Appl*, 1:73–85, 04 2015.
- [9] Jagdish Chandra and Paul Davis. Linear generalizations of Gronwall's inequality. *Proceedings of The American Mathematical Society PROC AMER MATH SOC*, 60, 10 1976.
- [10] Swetaprovo Chaudhuri, Saptarshi Basu, Prasenjit Kabi, Vishnu Rajasekharan Unni, and Abhishek Saha. Modeling the role of respiratory droplets in Covid-19 type pandemics. *Physics of Fluids*, 32:063309, 06 2020.
- [11] Swetaprovo Chaudhuri, Saptarshi Basu, and Abhishek Saha. Analyzing the dominant SARS-CoV-2 transmission routes toward an ab initio disease spread model. *Physics of Fluids*, 32:123306, 12 2020.
- [12] Sergio Chillón, Ainara Ugarte-Anero, Iñigo Iradi, Unai Fernandez-Gamiz, and Ekaitz Zulueta. Numerical modeling of the spread of cough saliva droplets in a calm confined space. *Mathematics*, 9:574, 03 2021.
- [13] Sandro Coriasco, Stevan Pilipović, and Dora Seleši. Solutions of hyperbolic stochastic PDEs on bounded and unbounded domains. *Journal of Fourier Analysis and Applications*, 27(77):42, 2021.
- [14] Jasmina Djordjević, Ivan Papić, and Nenad Šuvak. A two diffusion stochastic model for the spread of the new coronavirus SARS-CoV-2. Chaos Solitons & Fractals, 148:110991, 04 2021.
- [15] J Duguid. The size and the duration of air-carriage of respiratory droplets and droplet-nuclei. *The Journal of hygiene*, 44:471–9, 09 1946.
- [16] Mohamed El-Beltagy, Ahmed Etman, and Sroor Maged. Development of a fractional Wiener-Hermite expansion for analyzing the fractional stochastic models. *Chaos Solitons & Fractals*, 156, 03 2022.
- [17] Ignazio Maria Viola et al. Face coverings, aerosol dispersion and mitigation of virus transmission risk. *Engineering in Medicine* and Biology, 2:26–35, 2021.
- [18] Izrail Solomonovich Gradshteyn and Iosif Moiseevich Ryzhik. *Table of integrals, series, and products*. Elsevier/Academic Press, Amsterdam, seventh edition, 2007.
- [19] J Gupta, C.-H Lin, and Q Chen. Flow dynamics and characterization of a cough. Indoor air, 19:517–25, 07 2009.
- [20] Takeyuki Hida. White Noise: An Infinite Dimensional Calculus. Mathematics and Its Applications. Springer Netherlands, 1993.
- [21] Helge Holden, Bernt Øksendal, Jan Ubøe, and Tusheng Zhang. Stochastic Partial Differential Equations: A Modeling, White Noise Functional Approach. Springer Berlin Heidelberg, 2010.
- [22] Haojie Hou, Youguo Wang, Qiqing Zhai, and Xianli Sun. Optimal control of stochastic fractional rumor propagation model in activity-driven networks. *Applied Mathematical Modelling*, 142:115968, 2025.
- [23] Muhammad Khan, Zakia Hammouch, and Dumitru Baleanu. Modeling the dynamics of hepatitis E via the Caputo-Fabrizio derivative. *Mathematical Modelling of Natural Phenomena*, 14, 04 2019.
- [24] Tijana Levajković, Stevan Pilipović, Dora Seleši, and Milica Žigić. Stochastic evolution equations with multiplicative noise. *Electronic Journal of Probability*, 20(19):23, 2015.
- [25] Tijana Levajković, Stevan Pilipović, Dora Seleši, and Milica Žigić. Stochastic evolution equations with Wick-polynomial nonlinearities. *Electronic Journal of Probability*, 23(116):25, 2018.
- [26] Tijana Levajković, Stevan Pilipović, Dora Seleši, and Milica Žigić. Stochastic evolution equations with Wick-analytic nonlinearities, 2023.
- [27] Tijana Levajković and Dora Seleši. Malliavin calculus for generalized and test stochastic processes. *Filomat*, 31:4231–4259, 01 2017.
- [28] Chin-Lung Li, Chang-Yuan Cheng, and Chun-Hsien Li. Global dynamics of two-strain epidemic model with single-strain vaccination in complex networks. *Nonlinear Analysis: Real World Applications*, 69:103738, 02 2023.
- [29] Shichao Liu and Atila Novoselac. Transport of airborne particles from an unobstructed cough jet. Aerosol Science and Technology, 48, 11 2014.
- [30] Jorge Losada and Juan J. Nieto. Properties of a new fractional derivative without singular kernel. *Progress in Fractional Differentiation and Applications*, 1(2):87–92, 2015.
- [31] S. Lototsky, R. Mikulevicius, and B. Rozovsky. Intrusive and non-intrusive chaos approximation for a two-dimensional steady state Navier–Stokes system with random forcing. *Stochastics and Partial Differential Equations: Analysis and Computations*, 11, 01 2022.
- [32] S. Lototsky and B. Rozovsky. Classical and generalized solutions of fractional stochastic differential equations. *Stochastics and Partial Differential Equations: Analysis and Computations*, 8, 12 2020.
- [33] Benoit B. Mandelbrot and John W. van Ness. Fractional Brownian motions, fractional noises and applications. SIAM Review, 10:422–437, 1968.
- [34] Martin Maxey and James Riley. Equation of motion for a small rigid sphere in a nonuniform flow. *Phys. Fluids*, 26:883–889, 04 1983.
- [35] A.M Othman Omar, A. Reda Elbarkouky, and M. Hamdy Ahmed. Fractional stochastic modelling of COVID-19 under wide spread of vaccinations: Egyptian case study. Alexandria Engineering Journal, 61:8595–8609, 2022.
- [36] Manuel D. Ortigueira. Fractional Calculus for Scientists and Engineers. Springer, 2011.
- [37] Virender Panwar, P.S. Uduman, and J.F. Gómez-Aguilar. Mathematical modeling of coronavirus disease COVID-19 dynamics using CF and ABC non-singular fractional derivatives. *Chaos Solitons & Fractals*, 145:110757, 02 2021.
- [38] Mohammad Partohaghighi, Ali Akgül, Liliana Guran, and Monica Bota. Novel mathematical modelling of platelet-poor plasma arising in a blood coagulation system with the fractional Caputo–Fabrizio derivative. Symmetry, 14:1128, 05 2022.

- [39] Mati Rahman, Muhammad Arfan, Kamal Shah, and J.F. Gómez-Aguilar. Investigating a nonlinear dynamical model of COVID-19 disease under fuzzy Caputo, random and ABC fractional order derivative. Chaos, Solitons & Fractals, 140:110232, 08 2020.
- [40] Marco Rosti, Mattia Cavaiola, Stefano Olivieri, Agnese Seminara, and A. Mazzino. Turbulence role in the fate of virus-containing droplets in violent expiratory events. *Physical Review Research*, 3, 01 2021.
- [41] Ali Asghar Sedighi, Fariborz Haghighat, Fuzhan Nasiri, Shi-Jie Cao, and Chen Ren. Approaches in CFD modeling of respiratory droplet dispersion issues and challenges. Sustainable Cities and Society, 97:104696, 06 2023.
- [42] Dora Seleši and Stefan Tošić. The chaos expansion of fractional Brownian motion and fractional white noise with distributed order Hurst parameter, Preprint.
- [43] S.A. Seminara, M.I. Troparevsky, M.A. Fabio, and G. la Mura. Anomalous diffusion with Caputo-Fabrizio time derivative: an inverse problem. *Trends in Computational and Applied Mathematics*, 23(3), 2022.
- [44] Alireza Shadloo Jahromi, Omid Bavi, Mohammad Hossein Heydari, Masoud Koopaee, and Zakieh Avazzadeh. Dynamics of respiratory droplets carrying SARS-CoV-2 virus in closed atmosphere. Results in Physics, 19:103482, 10 2020.
- [45] Vasily E. Tarasov. Caputo–Fabrizio operator in terms of integer derivatives: memory or distributed lag? *Computational and Applied Mathematics*, 38(113):15, 2019.
- [46] Gilles Tissot, André Cavalieri, and Etienne Mémin. Stochastic linear modes in a turbulent channel flow. *Journal of Fluid Mechanics*, 912, 01 2020.
- [47] Nguyen Tuan, Nguyen Tuan, Donal O'Regan, and Vo Viet Tri. On the initial value problem for fractional Volterra integrodifferential equations with a Caputo Fabrizio derivative. *Mathematical Modelling of Natural Phenomena*, 16, 01 2021.
- [48] Duarte Valério, Manuel D. Ortigueira, and António M. Lopes. How many fractional derivatives are there? *Mathematics* 10(737):18, 2022.
- [49] Pratibha Verma and Dr Kumar. Analysis of a novel coronavirus (2019-nCOV) system with variable Caputo-Fabrizio fractional order. Chaos Solitons & Fractals, 142, 11 2020.
- [50] Ville Vuorinen, Mia Aarnio, Mikko Alava, Ville Alopaeus, Nina Atanasova, Mikko Auvinen, Nallannan Balasubramanian, Hadi Bordbar, Panu Erästö, Rafael Grande, Nick Hayward, Antti Hellsten, Simo Hostikka, Jyrki Hokkanen, Ossi Kaario, Aku Karvinen, Ilkka Kivistö, Marko Korhonen, Risto Kosonen, and Monika Österberg. Modelling aerosol transport and virus exposure with numerical simulations in relation to SARS-CoV-2 transmission by inhalation indoors. *Safety Science*, 130:104866, 06 2020.
- [51] Jim Walker, Justice Archer, Florence Gregson, Sarah Michel, Bryan Bzdek, and Jonathan Reid. Accurate representations of the microphysical processes occurring during the transport of exhaled aerosols and droplets. ACS Central Science, XXXX, 01 2021.
- [52] Hongping Wang, Zhaobin Li, Xin-Lei Zhang, Lixing Zhu, Yi Liu, and Shizhao Wang. The motion of respiratory droplets produced by coughing. *Physics of Fluids*, 32:125102, 12 2020.
- [53] Malia Zee, Angela Davis, Andrew Clark, Tateh Wu, Stephen Jones, Lindsay Waite, Joshua Cummins, and Nels Olson. Computational fluid dynamics modeling of cough transport in an aircraft cabin. *Scientific Reports*, 11, 12 2021.
- [54] Tusheng Zhang. Characterizations of the white noise test functionals and Hida distributions. *Stochastics and Stochastic Reports*, 41(1-2):71–87, 1992.